INTERNATIONAL JOURNAL OF HYDROGEN ENERGY 47 (2022) 8071–8090

Available online at www.sciencedirect.com

ScienceDirect

journal homepage: www.elsevier.com/locate/he

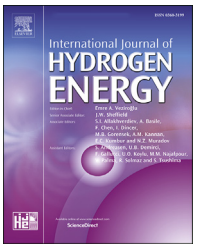

Review Article

From the perspective of new technology of blending hydrogen into natural gas pipelines transmission: Mechanism, experimental study, and suggestions for further work of hydrogen embrittlement in high-strength pipeline steels

Xia Wu [a], *Haifeng Zhang* [a,*], *Ming Yang* [b], *Wenlong Jia* [a], *Yazhou Qiu* [c], *Lan Lan* [a]

[a] *State Key Laboratory of Oil and Gas Reservoir Geology and Exploitation, Petroleum Engineering School, Southwest Petroleum University, Chengdu, Sichuan Province, 610500, China*
[b] *PipeChina Group Western Pipeline Co., Ltd., Urumqi, Xinjiang Province, 830000, China*
[c] *Shandong Haiyun Asphalt Co., Ltd., Binzhou, Shandong Province, 256500, China*

HIGHLIGHTS

- Reviewed the status of using high-strength pipeline steels to transport H_2.
- Discussed the latest progress and questions of HE mechanisms research.
- Described the blemishes of HE experimental research on pipeline steels.
- Proposed a new idea for the gas-phase hydrogen permeation experiment.
- It has given suggestions for the following work to study HE of pipeline steels.

ARTICLE INFO

Article history:
Received 5 September 2021
Received in revised form
10 November 2021
Accepted 11 December 2021
Available online 5 January 2022

Keywords:
Blending hydrogen into natural gas pipelines transmission
High-pressure
High-strength pipeline steel
Hydrogen embrittlement (HE) failure
Experimental study

ABSTRACT

Blending hydrogen into high-strength pipeline steels for high-pressure transmission may cause materials' hydrogen embrittlement (HE) failure. Although the hydrogen-induced failure of metallic materials has been studied for a long time, the process of hydrogen into the materials, hydrogen-induced delayed failure, and dynamic mechanisms of high-strength pipeline steels under high pressure have not been fully understood. This paper aims to provide a detailed review of the latest research on the hydrogen-induced failure of high-strength pipeline steels in hydrogen-blended natural gas transmission. First, introduced the typical hydrogen blending natural gas pipeline transmission projects and their associated research conclusions. Then, described the physical process of the HE in high-strength pipeline steels and the principle, development, and latest research progress of typical hydrogen embrittlement mechanisms in detail. Third, reviewed the research methods and progress of experimental and theoretical simulations for the HE in steels, including hydrogen permeation (HP) experiments, hydrogen content measurements, hydrogen distribution detection, mechanical property tests, and molecular dynamics

* *Corresponding author.*
E-mail address: xiawu-swpu@hotmail.com (H. Zhang).
https://doi.org/10.1016/j.ijhydene.2021.12.108

simulations. The shortcomings of existing experimental and theoretical simulation methods in the hydrogen-induced analysis of high-strength natural gas pipeline steels under high pressure are discussed. Finally, the future research directions and challenges of this problem are proposed from three aspects: the multimechanism synergy mechanism, the improvement of experimental methods, and the establishment of a new interatomic multiscale model.

Contents

Introduction

Hydrogen, the energy storage material of fuel cells and renewable energy, such as wind energy and solar energy, is becoming the fastest-growing energy carrier globally through more mature hydrogen fuel cells, wind hydrogen production, and solar hydrogen production technology [1]. China is expected to reach 100 billion m^3/a hydrogen production capacity in 2030, therefore consuming surplus renewable energy such as wind, water, and light and striving to achieve a carbon peak in 2030 and carbon neutrality in 2060. According to the European Green Deal, the EU makes hydrogen an ideal candidate on its way to a carbon-neutral economy in 2050 [2]. The American Fuel Cell and Hydrogen Energy Association (FCHEA) released "Road Map to A US Hydrogen Economy: Reducing Emissions and Driving Growth Across the Nation" to incorporate hydrogen into future energy development strategies in 2019 [3]. Relevant researchers have proposed that blending the prepared hydrogen into a natural gas pipeline through a particular volume concentration is best to transport hydrogen energy [4,5]. It can not only realize the long-distance and large-scale transmission and distribution of hydrogen energy but also save the investment cost and construction time of hydrogen pipelines and realize the goals of low costs and quickly opening up the whole industrial chain of hydrogen production, storage, transmission, and utilization [6,7]. In recent years, many countries have carried out demonstration projects of hydrogen-blended natural gas transmission in their natural gas pipelines and have a trend toward industrialization [8,9].

Once the hydrogen-blended transmission is implemented in natural gas pipelines, the pipes will be exposed to the hydrogen environment under different hydrogen concentrations for perennial. Under the action of pressure and flow, the hydrogen molecules in the pipelines will dissociate into H

atoms. The H atoms will enter the steels through adsorption and penetration to react with the atomic metal structure, resulting in microcrack propagation. Ultimately, the macro-mechanical properties of the pipes are deteriorated, resulting in a decrease in the fracture toughness of the pipes under the approved load-bearing conditions, namely, "hydrogen embrittlement (HE)" [10], which is a significant hazard.

Another tricky problem is that the current natural gas pipeline's high-pressure and high-strength characteristics will aggravate the HE phenomenon. According to the standard "API 5LX Specification for High-Test Line Pipe" and "Steel Pipes for Pipelines for the Transport of Combustible Fluids and Gases". Pipeline steels with yield strength ≥460 MPa can be classified as "high-strength steel". Following this definition, the existing pipeline steel grades of API 5L X70 (yield strength is 485 MPa) and above are high-strength pipeline steels. The steel for the backbone of the Alaska natural gas pipeline is X70 (7800 km, 8–10 MPa) [11]. X70 and X80 are primarily used in China's natural gas pipelines. According to statistics, the total length of X70 and X80 steels in China alone exceeds 30,000 km [12–14]. The China-central Asia natural gas pipeline, the longest gas pipeline globally, is mainly constructed by X70 steel. Part of them, whose length reached 800 km uses X80 steel [15,16]. Russia's Nord Stream 2 natural gas pipeline steel is also X70, with a design pressure of 22 MPa [17,18].

However, studies have shown that high-strength steel is more prone to hydrogen-induced delayed failure than low-grade steel [19–23]. This is because steels with greater yield strength have accumulated more significant elastic strain before plastic deformation. Therefore, the stress required for crack propagation is reduced, and the pipelines will also produce hydrogen-induced delayed fracture under a small external load. We usually classify X52 and above steels into the category of "high HE sensitivity" [24]. It can be seen that the existing natural gas pipelines are susceptible to hydrogen-induced failure. Subsequently, the solubility of hydrogen in steel obeys the Sievert law. The solubility is proportional to the square root of pressure, which indicates that the increase in pressure will increase the permeation amount of hydrogen in steel, resulting in the enrichment of H atoms in the maximum stress zone of steel and further increasing the HE sensitivity [25,26]. With the increasing number of hydrogen-blended natural gas pipeline transmission projects, high-strength steel faces a high risk of HE failure, which may lead to catastrophic consequences such as pipeline fractures, explosion, and combustion and seriously threaten the safe operation of hydrogen-blended natural gas pipelines.

Since Johnson [27] first reported that hydrogen would reduce the mechanical properties of metals, people have studied the phenomenon of metal embrittlement and developed and formed a series of mature research methods to explore the nature of HE. For example, hydrogen-containing metal specimens have been prepared by an electrochemical hydrogen charging method [28,29], a series of mechanical property tests were carried out on a universal testing machine or other equipment [30,31], the microstructure of the metal was observed by scanning electron microscopy [32], and H atoms were tracked and imaged by related technologies [33–35]. The interaction between hydrogen and metal microstructure is also described, several HE mechanisms are proposed to explain the embrittlement phenomenon. In recent years, benefitting from the rapid development of computers, molecular and atomic simulations have also provided new technical ideas for exploring HE. Despite many research bases, the hydrogen-induced failure of high-strength steels under high-pressure hydrogen-blended natural gas transmission is still a challenging problem. This is because the working conditions are more complex and involve different hydrogen partial pressure, pipes, and long-term hydrogen exposure. The experimental and theoretical research mentioned in the literature currently focuses on the conditions that do not match the actual operating conditions of the hydrogen-blended natural gas pipeline. The differences refer to the natural gas and hydrogen mixture's high pressure (10–15 MPa), while most experiments are conducted under conditions of lower pressure (<10 MPa). According to the previous research, the possibility of the high pressure promoting the penetration of hydrogen into the steel has not been fully understood. Besides, the high-grade pipeline steel used by the long-distance natural gas pipeline also introduces additional HE sensitivity. The published work still rarely focuses on this kind of material. Therefore, it is inaccurate if the current research results are directly used to assess the HE of hydrogen-blended natural gas pipelines without any improvement.

We did this review to clarify the differences between the existing experimental and theoretical research content and the operating conditions of hydrogen blending natural gas pipelines. Also, we further analyzed the urgently needed research which could solve the HE of hydrogen blending natural gas pipelines. This review would lead to a close connection between the theoretical research and the industrial applications, which is a more accurate prediction of the safe service limited duration of the pipeline. Besides, the following needed research in this field would also be understood according to our reviews.

This paper first briefly introduces some typical hydrogen-blended natural gas transmission projects worldwide and analyzes the shortcomings of some supporting research. In the third chapter, the physical process and existing mechanisms of the HE failure are emphatically introduced, and the discussion of some different viewpoints in the literature. The fourth chapter reviews typical hydrogen charging experiments, hydrogen content measurements, hydrogen distribution detection, mechanical property experiments, and molecular simulation experiments and proposes suggestions for further work. This workflow needs to be improved to understand the hydrogen-induced failure process of high-strength steels under hydrogen blending natural gas conditions with more appropriate and accurate experimental methods.

Typical projects and their associated research

One way to obtain hydrogen is to produce hydrogen by the electrolysis of water from renewable energy such as wind energy and light energy [36,37]. Because hydrogen is not suitable for massive use as fuel, it is more commonly used as an energy [38] carrier or transportation energy to achieve energy conversion and efficient use (such as hydrogen fuel cells),

which forms a hydrogen energy utilization route (Fig. 1). Given this, relevant researchers [4] suggest that the prepared hydrogen should be blended into the natural gas pipeline in a particular proportion, rather than necessitating the unique construction of a hydrogen pipeline, which is the most economical means for the long-distance transportation of hydrogen at present. There are already successful industrial projects (Table 1) in Europe, America, and other countries.

Because of the significant physical differences between natural gas and hydrogen, before implementing the hydrogen blending project, the relevant institutions carried out many supporting studies to analyze the feasibility of the hydrogen blending operation of natural gas pipelines. For example, the VG2 project in the Netherlands focuses on the terminal of hydrogenated natural gas. It obtains a hydrogen-blended volume ratio range of less than 5% on the premise of safe use at the user side. The NaturalHy [60,61] project funded by the EU believes that hydrogen charging reduces the safety distance of pipeline explosion but increases the risk around the explosion. The HYREADY [62] project initiated by DNV-GL considers the adaptability of transmission systems, gas distribution systems, user terminals, and hydrogen filling facilities at different hydrogen concentrations. In addition, the Gas Technology Institute (GTI) and the Department of Energy (DOE) of the United States are also paying attention to the research and development of pure hydrogen pipelines [63,64].

However, at present, systematic research on the HE of hydrogen-blended natural gas pipeline steels is rarely mentioned. It is reported [62,65] that when the hydrogen content is 0–20% (volume content), the impact on the safety of natural gas pipelines is relatively tiny. Nevertheless, it is worth noting that most of the natural gas pipelines in Europe, the United States, and other countries that implement hydrogen-blended transportation are natural gas distribution pipelines or old pipelines. The essential characteristics of these pipelines are short conveying distances (tens of kilometers), low conveying pressures (0.2–0.35 MPa), and a low steel grade of pipeline steel (often using API 5L X42 and X46 steel, yield strength in 310 MPa below). The above studies also pointed out that so-called safety means low-strength pipeline steel is not sensitive to hydrogen exposure under low pressure.

It is undeniable that these studies have reference significance for developing hydrogen-blended natural gas transmission but are not fully applicable. Because according to the data, the maximum transmission pressure of international natural gas pipelines has developed from approximately 6 MPa in the 1960s to 15–20 MPa at present, and pipes have also developed from grade X52 steel, gradually increasing to the current X80 steel grade (even a tiny amount of X100, X120) [66–69]. These data show that the transmission pressure of natural gas pipelines and the steel grade of materials gradually increase. The old natural gas pipelines in most areas will be updated. It is foreseeable that the application scale of high-pressure, high-strength natural gas pipeline steels will become more prominent. For example, one of the Nord Stream 2 natural gas pipeline plans uses this pipeline to transport H_2 [17]. In addition to the pressure, steel grade, and scale problems, the hydrogen exposure time in the actual pipeline is particularly long, and the operation is not as controllable as the experiment. Therefore, under this trend, the research of hydrogen-blended natural gas transmission technology should fully consider the pipeline's HE sensitivity under this working condition. A more extensive systematic study may be required to understand the effect of hydrogen-blended natural gas, mainly hydrogen, on the properties of high-strength pipeline steels.

Hydrogen embrittlement in high-strength steels

This chapter will discuss the complex process of the hydrogen-induced failure of high-strength steels to understand HE. This process involves infiltration, diffusion and effect of hydrogen. The HE mechanism describes the kinetic details of the interaction between hydrogen and the metal microstructure. Despite various HE mechanisms reported to explain the phenomenon, there is no unified understanding. Many problems are still under discussion.

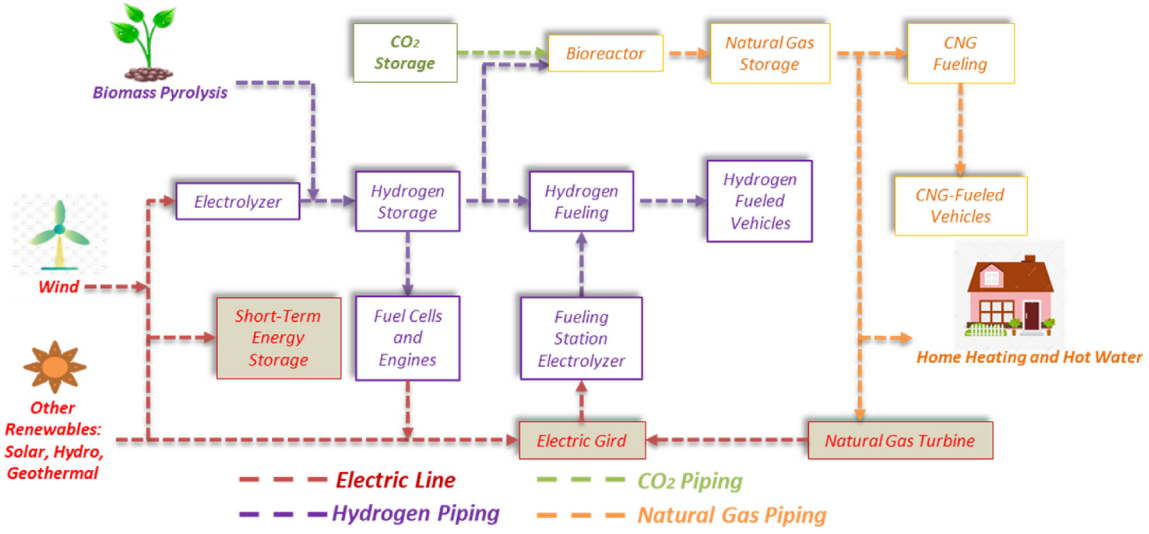

Fig. 1 – Hydrogen applications road map.

Table 1 – Typical examples of blending hydrogen into the natural gas pipelines transmission projects worldwide.

Projects in production	Country	Production time	Project situation
WindGas Falkenhagen [39,40]	Germany	2011	The hydrogen content is unknown. The hydrogen produced by 2 MW wind turbine is mixed into the natural gas distribution network of ONTRAS Gas Operation Company in Germany
ITM Power/Mainova/NRM Thuqa plant [41–43]	Germany	2013	Mixing hydrogen <2%, at 3.5 bar without compressor
Network management by injecting hydrogen to reduce carbon content (GRHYD) [44,45]	France	2013	2013–2015: Trial operation phase, providing hydrogen-blended natural gas for natural gas-powered vehicles 2016–2020: Five-year operation phase, filling up to 20% hydrogen into the natural gas distribution network
P2G Ibbenbüren demonstration plant (RWE) [46–48]	Germany	2014	The hydrogen content is unknown. The hydrogen produced by the 150 kW electric unit is mixed into the natural gas distribution network belonging to The German Westnetz Gas Operation Company
Energiepark Mainz [49,50]	Germany	2015	With hydrogen content of 0–15% and pressure of 6–8 bar, it was mixed into a short pipeline
P2G NFCRC Phase 2 @ UCI [51,52]	America	2016	The hydrogen content is 0–3.4%, and the hydrogen mixture is transported from 2.1 bar to 2.8 bar in the 4-inch pipe
HyDeploy [53,54]	Britain	2016	With an unknown amount of hydrogen, hydrogen produced by 0.5 MW electrical units was injected into the UK gas network
ENGIE GRHYD [44,45]	France	2018	Add 10% hydrogen to the gas pipeline network of 100 new residential communities for a demonstration period of two years from 2018 (to be increased to 20% by 2020).
Wind to Gas Brunsbuttel [55,56]	Germany	2019	The hydrogen content is 0–2% to provide hydrogen-containing natural gas to natural gas filling stations
ITM Power HyDeploy [53,57]	Britain	2019	Mixing hydrogen 0–20%
Snam [58,59]	Italy	2019	Mixing hydrogen 5%

Procedure and influencing factors of hydrogen embrittlement

As shown in Fig. 2. Under the high operation pressures, the hydrogen in mixed natural gas would dissociate into H atoms by the process of adsorption and desorption on the surface of the pipeline steel [65,70]. As the smallest atom in nature, H atoms can easily go across the micro-gap on the steel surface and be captured by the microstructure of the steel, such as dislocations and vacancies. The H atoms then would desorb and migrate along the lattice defects. Under this situation, in the presence of external stress, which could be from residual stress, local plastic deformation, micro-pore accumulation,

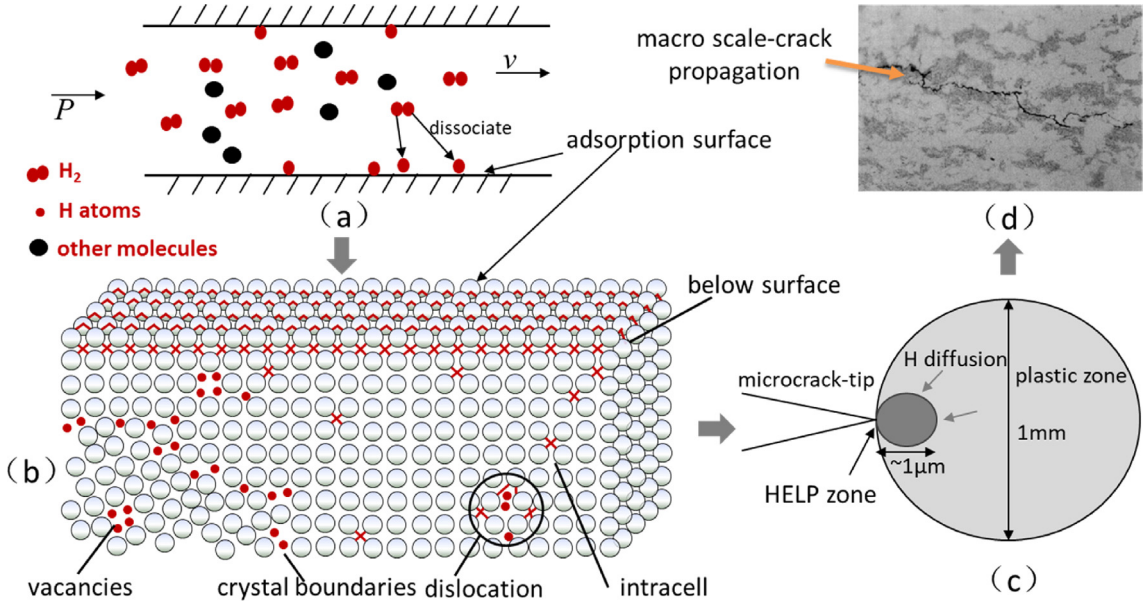

Fig. 2 – Physical process of hydrogen embrittlement: from micro to macro, (a) hydrogen is dissociated into H atoms in the pipelines and adsorbed to the inner surface of the metals, (b) H atoms or regenerated hydrogen molecules degrade metal lattices, (c) hydrogen breaks the lattices and evolves into micro-crack propagation, and (d) macroscopically visible cracks appear.

and micro-crack propagation, could be formed in the steel microstructure [71,72]. Then the overall macro-mechanical properties of the steel, such as yield strength, toughness, fatigue resistance, are degraded. The unexpected failure of the steel will occur before its service life is reached. This is a multiscale coupling process, starting from hydrogen's entry, which induces local cracks on the mesoscopic scale and finally causes the macroscopic failure of pipeline steels.

After the hydrogen enters, the hydrogen entering the material is divided into two types: 1) diffusion hydrogen that moves or jumps between lattices in the form of atoms, and 2) trap hydrogen that is captured by crystal defects (such as vacancies and impurities) [73–75]. Diffusion hydrogen may reform hydrogen molecules, generate hydrogen pressure, form load action inside the material, and degrade the microstructure of the metal. Trap hydrogen generally does not leave, but some hydrogen will escape from the trap and form free H atoms again under the change of thermodynamic energy. If the energy change is significant enough, it will escape from the metal interior and return to the external environment. Nevertheless, no matter what form of hydrogen exists in the material, it can participate in the hydrogen-induced failure process of the material.

Reports show that there may be two types of internal degrade processes of hydrogen-induced failure. 1) If there were additional stress, it would force the hydrogen gathering at the crack tip. The enriched hydrogen in the narrow space accumulated to a particular hydrogen partial pressure that may degrade the atomic metal bond and form the supersaturated vacancy group. The microcrack then propagates at the crack tip under the load of the hydrogen partial pressure [76]. 2) If there is no additional stress, the hydrogen molecules reformed inside the material will also be gathered. The generated hydrogen partial pressure will then drive the crack propagation. It should be noted that although the cracks can propagate to a certain extent, the propagation speed is relatively lower than that of the cracks faced external loads [77]. Ahn et al. [78] found that hydrogen reduced the fracture toughness of the material by 70% by promoting the growth and coalescence of multiple micropores at the crack tip. Neeraj et al. [79] also found high-density dislocations and vast amounts of nanopores under the fracture surface of the specimen in the hydrogen environment, indicating that hydrogen promoted the initiation and propagation of cracks in the steel.

The complex activity of hydrogen in the material first degrades the material's microstructure and then leads to macroscopic failure. The failure degree depends on the external environment and the internal situation of the metal. Under the condition of hydrogen-blended natural gas transmission, the external factors are the changes of hydrogen partial pressure, temperature, flow rate, and pipeline operating pressure. Because this will affect the amount of hydrogen dissolved, the more hydrogen content, the more serious the HE [80]. The internal factors are the microstructure of metal, such as inclusions, grain boundaries, and vacancies, which will affect the amount of hydrogen captured and stimulate different kinetic mechanisms, then affect the HE effect [81,82].

Description of hydrogen embrittlement mechanisms

To understand the movement of hydrogen in steel and its failure process, a variety of machine models have been reported to explain the HE in steel. Among them, the mechanism model with high recognition includes the following 1) hydrogen pressure theory (HPT), 2) hydrogen-enhanced decohesion mechanism (HEDE), 3) adsorption-induced dislocation emission (AIDE), 4) hydrogen-enhanced local plasticity (HELP), and 5) hydrogen-enhanced strain-induced vacancy formation (HESIV) [83].

Hydrogen pressure theory (HPT)

In 1941, Zapffe et al. [84] proposed HPT. The theory suggests that H atoms will be separated from defects such as micropores or inclusions after entering the metal, while the locally accumulated H atoms will combine into hydrogen molecules. With the increase in hydrogen molecules, a high hydrogen pressure is generated. When the local hydrogen pressure exceeds the critical strength of the material, hydrogen-induced cracking occurs. The deeper explanation is that the hydrogen pressure forms a load in the metal. As the pressure increases until the atomic bond in the local region breaks, the crack propagation is driven to the long ladder crack and accelerates the process [85]. Bae et al. [86] observed that the penetrated hydrogen quickly moved to the micropore position to generate expansion in a high-pressure hydrogen environment, which accelerated the propagation of microcracks and led to quasi-cleavage fracture accompanied by tensile deformation, indirectly proving HPT. HPT is based on experimental and theoretical derivations. Without an external load, internal stress, and constraint, the load effect of hydrogen pressure may be the main reason for HE, which can well explain hydrogen-induced cracking and hydrogen bubbling [85].

Nevertheless, it is worth noting that the hydrogen pressure is challenging to measure directly by the sampling method. The dynamic thermodynamic equilibrium conditions between the hydrogen pressure in the defect and the diffusion of hydrogen around the defect must be calculated [87]. When only considering the hydrogen pressure effect without the embrittlement of diffusion hydrogen, the calculated hydrogen is often higher than the stress intensity required for fracture, reaching the GPa order of magnitudes [85], which is inconsistent with the actual situation needs further discussion.

Hydrogen-enhanced decohesion mechanism (HEDE)

HEDE is also known as hydrogen-induced decohesion (HID). In 1926, Pfeil [88] proposed hydrogen-induced intermolecular bond energy reduction inference according to experimental results. Afterward, Gerbrich et al. [89] refined this inference to the HEDE mechanism, which mechanism suggests that the trapping of H atoms by the metal lattice will reduce the cohesive local strength between the lattice surface and the metal atoms and cause the atomic bond to fracture under low stress so that the microcracks easily nucleate and propagate, leading to the macroscopic failure of the material. This theory can well explain the intercrystalline fracture observed in high-strength steel. Nevertheless, at present, no experiment can directly prove the correctness of this theory [90]. The

observation and theoretical calculation of intercrystalline fractures [91–94] support the HEDE mechanism. However, the controversial point is that some researchers believe that the electrons of H atoms increase the repulsion between metal atoms [95–97]. This is because the electrons of H atoms tend to enter the d-band of the metal atomic nucleus. The overlap of this d-band determines the repulsion between metal atoms. The entry of the hydrogen's electrons increases the repulsive force between the metal atmos and reduces the cohesive strength of the crystal lattice.

Nevertheless, suppose the H atoms are uniformly distributed in the microstructure. In that case, the significant debonding effect will not be caused due to its minimal solubility. Furthermore, the occurrence of the HEDE mechanism depends on pressure conditions and hydrogen content. However, this theory does not discuss why a particular hydrogen concentration and a necessary condition are needed.

Adsorption-induced dislocation emission (AIDE)

In 1972, Beachem [98] creatively used carbon atom rearrangement technology to observe the crack surface of the HE fracture of steel by TEM and found that under the condition of a high-stress intensity factor, there were large amounts of pits on the crack surface. It is shown that the aggregation of micropores is the cause of crack propagation under this condition, which inspires the proposal of the AIDE mechanism. In 1979, Lynch [99] pointed out in his published paper that dislocation nucleation was formed through the fracture and regeneration of atomic bonds, while the hydrogen adsorbed at the crack tip weakened the atomic bond energy, thus promoting dislocation emission. Finally, the nucleation and growth of micropores at the crack tip led to crack propagation, which formally proposed the AIDE mechanism. The mechanism suggests that hydrogen adsorbed on the surface strongly affects the surface energy and further promotes or inhibits dislocation nucleation, supported by relevant reports [100–102]. In the AIDE mechanism, the term "dislocation emission" refers to the whole process of dislocation nucleation away from the crack tip. The nucleation stage is crucial by breaking and reforming the interatomic bond at several atomic distances and simultaneously forming dislocation cores and surface steps. At the same time, the adsorbed H can weaken the interatomic bond, promoting nucleation. When hydrogen enters the material to produce this effect, significant dislocation activities lead to crack propagation because dislocation emission produces crack propulsion. However, direct evidence of this phenomenon is not yet available.

Furthermore, in the AIDE mechanism, crack propagation is caused by dislocation emission at the crack tip and the nucleation and growth of micropores at the crack tip. Nevertheless, in the HELP mechanism, crack propagation is promoted by the enhanced dislocation mobility near the crack tip. There are different opinions, and further discussion is needed.

Hydrogen-enhanced local plasticity (HELP)

As mentioned above, Beachem [98] also found in the experiment that with the gradual decrease of the stress intensity factor, the plastic deformation of cracks gradually transformed into the quasi-fracture mode. It finally became an intergranular fracture under the lowest stress intensity factor, which promoted the proposal and development of the HELP mechanism [103]. Based on the in situ transmission electron microscopy method, Birnbaum et al. [104] further observed the interaction between dislocations and hydrogen at the crack. The results showed that hydrogen segregation occurred at the dislocation site of the metal. The degree of segregation was related to the strain rate and temperature. Birnbaum speculated that the segregation of hydrogen led to the formation of the Cottrell atmosphere at the dislocation, thereby reducing the metal strength and causing plastic deformation, which indirectly confirmed the accuracy of the HELP theory. The HELP mechanism suggests that the deterioration of steel properties is due to increased dislocation mobility because of hydrogen. In this process, hydrogen has a shielding effect on the elastic stress field of dislocations, thereby enhancing the mobility and slip positioning of dislocations and reducing the stress value required for local plastic deformation. This phenomenon is also called the "softening effect". The HELP theory can explain the hydrogen-induced cracking phenomenon observed by Beachem in the experiment driven by the plastic deformation at the crack tip [98]. Other experiments have shown that in a hydrogen environment, dislocation mobility in metal indeed increased [105].

Nevertheless, this theory is also challenged by many experimental conclusions. For example, the HELP theory suggests that hydrogen should reach the crack tip first so that the base metal before the crack tip softens and the crack extends. However, the experiment shows that the crack propagation speed may be much greater than the diffusion speed of hydrogen in the metal [106]. Therefore, it is generally believed that the HELP mechanism needs to cooperate with other mechanisms to eventually deteriorate steel performance in a hydrogen environment [107].

Hydrogen-enhanced strain-induced vacancy formation (HESIV)

In 2001, Nagumo [108] analyzed the TDA results and found that H atoms were more easily trapped by vacancies, indicating a synergistic effect between hydrogen and vacancies. He formally proposed the HESIV mechanism in 2004 [109]. The mechanism suggests that the hydrogen environment will enhance the density and aggregation of the vacancy. When the vacancy agglomerates into micropores and the micropores merge into large pores, the ductile crack propagation resistance of the steel will decrease, which leads to crack propagation. Further analysis by Hickel et al. [110] found that the energy of hydrogen in the vacancy would be reduced, so it was conducive to the formation of micropores, which further confirmed the HESIV mechanism. Nagumo found that the hydrogen-containing specimens had high pore density by comparing the cross-sectional micrographs of the fatigue fracture specimens under the hydrogen/nonhydrogen experimental conditions (Fig. 3) [109]. In other experiments using cast iron and alloys, a similar increase in pore density was also observed [111], indicating that the HESIV theory plays a critical role in explaining the properties of hydrogen-induced steels. Nevertheless, since the HESIV theory is based on the premise that there is a local plastic zone at the crack tip, it cannot explain the cause of the plastic zone. Therefore, it is generally

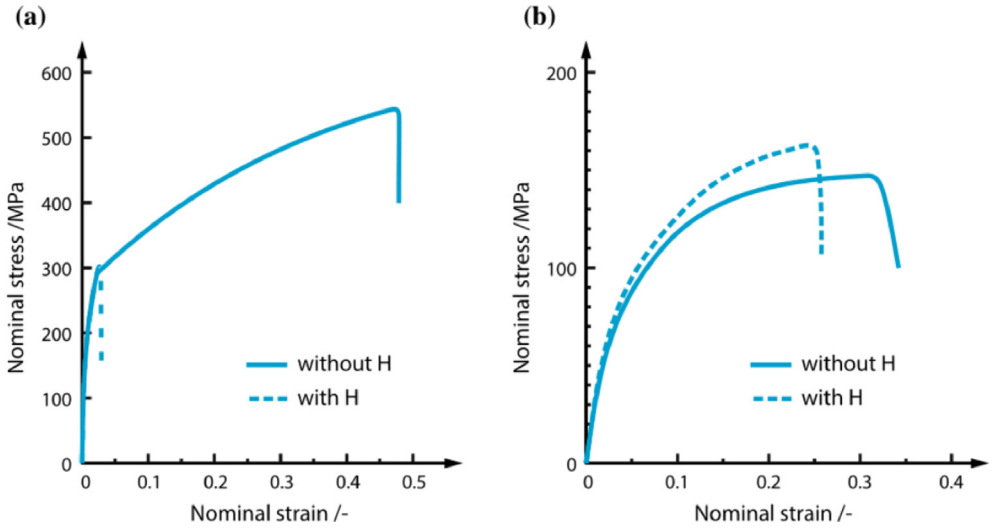

Fig. 3 – Stress–stress data from tensile testing of hydrogen-charged and uncharged specimens of (a) nickel-based alloy 625, (b) iron [109].

believed that the HESIV theory also needs to be combined with other mechanisms to explain the overall process of steel performance degradation [96,112].

Discussion

It can be seen that although some HE mechanisms have been proposed to explain the process of hydrogen degradation of the metal microstructure, there are some contradictory views between the mechanisms and the mechanism itself has problems that cannot be clarified. Moreover, several challenging issues in the report need to be discussed. 1) The HPT cannot explain hydrogen-induced reversible damage. For example, in a macroscopic tensile experiment, hydrogen inhibits plastic deformation and changes the fracture morphology from toughness to brittleness [113,114]. This shows that the behavior of hydrogen in materials cannot be explained by hydrogen pressure theory alone. 2) The Mn, S, P, and other elements can also debond the interface. The report [95] questioned whether hydrogen would cause the interface to debond and indirectly doubted the accuracy of the HEDE mechanism. 3) The root cause of crack propagation in the AIDE mechanism is unclear, and 4) regarding the HELP mechanism, Song et al. [115] questioned whether the increase of dislocation mobility was caused by hydrogen because they found that hydrogen inhibited the movement of an edge dislocation in iron under H Cottrell gas conditions.

Although the description of the HE mechanisms is still controversial, in general, the academic community is increasingly convinced that the synergy of various mechanisms is the cause of the degradation of steel performance in a hydrogen environment. For example, the effect of the HELP mechanism reduces the back stress required for dislocation emission, which makes the dislocation nucleation by the AIDE mechanism at the crack tip easier to move [116]. In addition, for the crack propagation dominated by the AIDE mechanism, the HELP or HEDE mechanism will make the vacancy in front of the crack nucleate more efficiently, thus promoting dislocation formation [117]. Videlicet, with the help of the HELP and HEDE mechanisms, the AIDE mechanism is more likely to occur. It should be noted that no experiment can directly prove the accuracy of either a single theory or a combination of theories; therefore, there is no conclusion on the applicable conditions of various theoretical methods.

Experimental study on hydrogen embrittlement of high-strength steels

In this chapter, we will discuss a series of experimental methods used to understand the hydrogen-induced failure of steels. Corresponding to the process of hydrogen entering the materials, diffusion, aggregation, and degradation of the microstructure, the hydrogen charging experiments, hydrogen content measurement, hydrogen distribution detection, mechanical property measurement, and molecular simulation experiments are reviewed. Microscopic observation can provide hydrogen motion information, while molecular simulation further promotes the development of the HE mechanism. Through these experiments, the gradual process of HE can be observed, and the effects of different hydrogen contents, pressures, and exposure times on the HE procedure can be understood.

Hydrogen permeation experiments

Hydrogen entering the pipes is the beginning of HE. When hydrogen molecules are dissociated into H atoms, they are adsorbed on the metal surface or penetrate the metal to remain. The mechanical properties deteriorate by interacting with the metal microstructure. The HP experiment aims to obtain hydrogen-containing metal specimens for further microscopic research.

Electrochemical hydrogen charging is the most commonly used hydrogen charging experimental method. In 1962, Devanathan and Stachurski [118] proposed a double-cell electrochemical hydrogen charging method (D-S dual battery) in their research. This experimental device comprises two electrochemical batteries with the same structure, the hydrogen charging terminal is the cathode to produce hydrogen or other gases, and the oxidation terminal is the anode to oxidize the target gas. A hydrogen filling solution (usually sulfuric acid or salt solution) is added to the cathode, and a particular poisoning agent is added to inhibit the binding of H atoms to hydrogen molecules. According to Fick's second law, H atoms diffuse from the cathode to the anode, and the electrons lost in the anode are oxidized to hydrogen ions, resulting in a hydrogen permeation current [119], which two formulas can express:

$$H^+ + e^- \rightarrow H \quad (1)$$

$$H - e^- \rightarrow H^+ \quad (2)$$

In the 1980s, Choo [120] and Archer et al. [121] used the electrochemical hydrogen charging method in their papers published in the same year, and a D-S dual battery carried out the experimental design. Their current density was between 0–2.34 mA/cm^2, the specimen thickness was between 0.06–3 mm, the test environment was average temperature and pressure, and the equipment was not significantly changed. Recently, Thomas et al. [122] further improved the experimental device and process based on the experiments of Devanathan and Stachurski (Fig. 4). The main change was to use inert argon to drive the battery, thus removing oxygen mixing. The experimental results show that a higher experimental voltage and a more stable oxidation current can be obtained under this condition. Another improvement is to carefully control the hydrogen permeation current to slow down the diffusion rate of hydrogen in the sample [123–125]. This is helpful to observe the gradual process of hydrogen movement in the samples. The use of the different currents can obtain a comparative analysis of the HE process. Timing Zhang et al. [126–128] used two improved hydrogen charging tests to explore the hydrogen concentration on the secondary surface of high-strength steel (X80, X100). Their improvements were as follows 1) the thermostat was added to observe the effect of temperature on the hydrogen charging process, and 2) the experimental pressure was increased from atmospheric pressure to 11.56 MPa by autoclave.

Electrochemical hydrogen charging is the most widely used method in the study of hydrogen corrosion of metals. However, its working conditions are inconsistent with hydrogen-blended pipelines transmission. The limitations of the electrochemical hydrogen charging method are as follows. 1) Although adding the poisoning agents can inhibit hydrogen ions from forming hydrogen molecules to obtain more hydrogen atoms. There is no quantitative standard for the exact amount of inhibitor that needs to be used. The mechanism and quantitative relationship of the inhibitory effect of poisoning agents with current changes have also not been discussed carefully. 2) As stated in the HEDE mechanism, electrons may reduce the cohesive energy of the metal lattice. In the process of electrochemical tests, the electrons in the electrolyte may also degrade the properties of the metal. Therefore, the metal degradation results obtained through electrochemical tests may not be all caused by the measured H atoms. 3) The penetration of H atoms into the metals in the electrochemical system is driven by electrons (free electrons attract hydrogen electrons and form H atoms). However, the penetration of H atoms in the hydrogen-blended pipelines is due to pressure, flow rate, or other reasons.

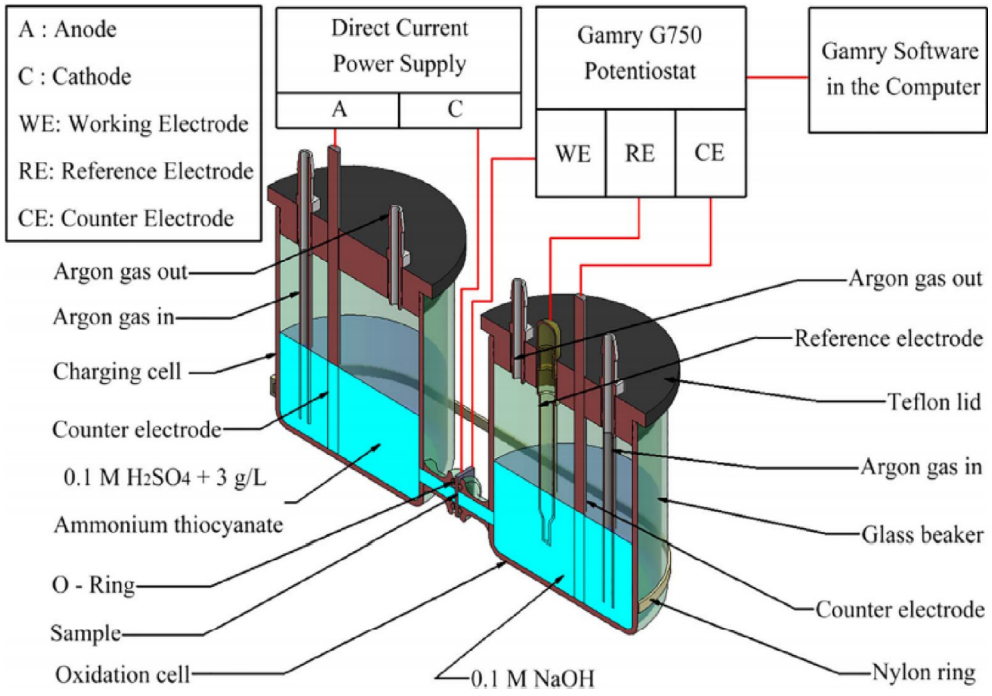

Fig. 4 – Electrochemical HP test setup [122].

For the study of HE in hydrogen-blended pipeline steels, some hydrogen permeation experiments in gas-phase environments can provide a reference. Shuai Zhang et al. [129] used an in situ hydrogen charging experiment method. The pressure vessel was vacuumed first, then purged three times with nitrogen. Finally, a set amount of hydrogen was added, and the equilibrium pressure reached 12 MPa. The experiments carried out by Thanh et al. [31] on small punches also showed hydrogen exposure behavior, the hydrogen permeation experiments were carried out in a mixture of hydrogen and natural gas at three pressure levels (5, 7, and 10 MPa), five hydrogen fractions (0.1%, 0.5%, 1%, 3%, 5%), and an exposure time of 0.5 h. Furthermore, the gas environment of the two air and pure hydrogen groups was used for comparative analysis. This is quite different from the experiment of Shuai et al. They compared the effects of different pressures and hydrogen contents on the HE sensitivity of the tube, which is more in line with the actual working conditions. However, the shortcoming is that the exposure time is too short, and hydrogen exposure behavior may not reach saturation. Zhou et al. [30] reported that the hydrogen partial pressures in the universal testing machine were 0%, 1.0%, 2.2%, and 5%. This achieved the requirements of different hydrogen partial pressures, but the constant total pressure of 12 MPa did not reflect the influence of pressure change on the hydrogen osmotic process of the pipes.

It can be seen that these gas-phase HP experiments have certain shortcomings, which may be due to the equipment. These types of equipment are all in a small closed space. Although the pressure and hydrogen content can be controlled, the flow conditions in actual working conditions cannot be obtained. The hydrogen exposure process of high-strength pipeline steels occurs under gas-phase high pressure considering only the effect of hydrogen addition on the HE process. The hydrogen in the actual pipelines is in a flow state, and molecular collision under high pressure may be the main reason for affecting the hydrogen dissolved quantity. Therefore, from an experimental point of view, the hydrogen permeation experiment system needs to be updated. This requires a vast closed-loop system, including high-strength pipelines, valves, compressors, hydrogenation machines and other equipment. This system can provide gas flow conditions and be equipped with sophisticated measuring instruments to read data accurately, and can take into account the requirements of pressure, hydrogen content, flow conditions, and exposure time. In this way, it is convenient to accurately measure the accurate hydrogen content of the pipe under the corresponding conditions and then evaluate the influence of these parameters on the HE process.

Hydrogen content measurement

Charge hydrogen by electrochemical method, the current density can accurately obtain the hydrogen content. If gaseous hydrogen charging experimental occurs, the most used method is thermal desorption analysis (TDA).

After gaseous hydrogen charging, the specimens were put into a tube furnace connected to the gas chromatograph to detect the amount of hydrogen released. To ensure the hydrogen is thoroughly discharged, the specimens are heated at a constant rate, and the hydrogen in the metals is gradually released during the heating process. The hydrogen escape rate curve can be obtained according to the temperature and the escape rate of hydrogen. The horizontal axis of this curve is the temperature, and the vertical axis is the hydrogen escape rate (wppm/s). With the change of temperature, the curve may show two peaks. The first peak at the relatively low temperature represents the rate of hydrogen escaping from weak traps. The second peak at the relatively high temperature represents the rate of hydrogen escaping from solid traps. From this curve, researchers can see that the temperature at which hydrogen begins to escape is when the hydrogen escape rate is more significant than zero. The temperature at which the lower desorption peak appears is the escape temperature of irreversible hydrogen. When the hydrogen evolution rate approaches zero again and no longer changes with time and temperature, it can be determined that the reversible hydrogen in the sample is finally released, that is, degassing. The kinetic model proposed by Choo et al. [130] can be used to analyze the results. The detrapping activation energy is determined from the peak temperature T_P, and the following equation gives the desorption kinetics:

$$\frac{\partial X}{\partial t} = A(1-X)\exp\left(\frac{-E_a}{RT}\right) \tag{3}$$

In this equation, X is the hydrogen desorption content, t is time, A is a constant, E_a is the desorption activation energy, T is the thermodynamic temperature, and R is the ideal gas constant. If the heating rate is constant φ, the maximum desorption rate occurs when the derivative of Equation (3) is zero. The calculation of trap energy is given as follows:

$$\frac{\partial\left(\varphi/T_p^2\right)}{\partial\left(1/T_p\right)} = \frac{-E_a}{R} \tag{4}$$

Many reports [131–139] use reaction kinetics models to analyze TDA results, which show that quantitative data of H concentration can be obtained by TDA analysis. Subsequently, the types of hydrogen traps and the ability to capture H in steel can be analyzed by the height and position of the H escape peaks. Combined with transmission electron microscopy, the change in microstructure in steel can be judged. The dissolved amount of hydrogen under different experimental parameters can be obtained by analyzing the results of gas-phase hydrogen charging experiments with the TDA method. The relationship between the number of hydrogen trapped and different pressures, exposure times, and hydrogen contents can be inferred and how these parameters affect the hydrogen trapped to capture hydrogen.

There is a problem that needs to be noted. Before the TDA test, there was a vacuum process in which H trapped in traps with lower binding energy was easily desorbed from the specimens at room temperature. The reports [140,141] provided ways to mitigate this phenomenon. Furthermore, the specimen size will also affect the results [142], so designing a reasonable specimen size before the experiment.

Hydrogen distribution detection

Observing the distribution information of hydrogen in the high-strength steels can infer the joint movement of hydrogen

and the pipes, which helps to understand the dynamic process of hydrogen in the metals. At present, a variety of indirect imaging methods and their combination methods have been proposed to detect the hydrogen distribution. The commonly used observation techniques include 1) the 3D Atom probe (3DAP), 2) the scanning transmission electron microscope (STEM) or scanning electron microscope (SEM), 3) the scanning Kelvin probe force microscope (SKPFM), 4) secondary ion mass spectrometry (SIMS), and 5) the hydrogen microprinting technique (HMT) [143–146].

3DAP, also known as atom probe tomography (APT) [147], can map the nano-space distribution of atoms in metal specimens by analyzing and identifying atoms in each position of the material one by one [148]. In the process of atom-by-atom analysis, 3DAP can understand the uneven distribution of different alloy elements in the microregions of metal materials and explore the segregation distribution of alloy elements at various interfaces and crystal defects. Moreover, observation data at the microscale can be effectively provided by combining transmission electron microscopy (TEM) technology [149–151]. Jiang et al. [152] found that H was mainly trapped in the carbides at the grain boundary and matrix interface of AISI 4140 steel by using this technology. Fan et al. [153] believed that the capture site of H was in the inversion austenite. From the experiment of Takahashi et al. [33–35], it can be found that the capture position of deuterium atoms in the vanadium carbide precipitation phase was not consistent, so it was challenging to confirm the optimal capture position of hydrogen.

STEM is equipped with STEM accessories based on TEM. Its working principle is that the electron beam is converted into a small beam spot and focused on the surface of the specimen through a series of coils. Then the beam spot is accurately controlled by the scanning coil to scan point by point on the thin specimen to form a scanning transmission electron image (STEM image) [154]. Nevertheless, TEM can only form a micromorphology diagram, which cannot be used for generalized hydrogen imaging [96]. A small number of researchers have achieved hydrogen imaging on graphene films [155], but harsh experimental conditions are difficult to achieve in the microscopic imaging of pipeline steel.

SKPFM was developed based on atomic force microscopy (AFM) combined with the macroscopic Kelvin method. The distribution of H and the trend of H changing with time were characterized by measuring the small potential change on the material surface. Wang et al. [156] used this method to charge hydrogen in cracked specimens and found that H was enriched at the crack tip, and the crack tip potential also changed. After H diffusion away from the tip, the potential gradually recovered. Li [157] and Guo et al. [158] found that the preferential nucleation sites of the specimen to be tested changed because of hydrogen charging. Therefore, SKPFM was used to accurately infer the enrichment of H and the pitting nucleation caused by it. The surface potential of the specimen can be obtained by SKPFM scanning, but it is greatly affected by the surface roughness and microstructure.

The principle of SIMS is to use the focused ion beam to bombard the specimen surface to sputter out the secondary ions, then use the detector to detect the flight time of ions and carry out mass spectrometry separation and analysis according to the mass-to-charge ratio. Finally, the elemental composition and distribution of the specimen surface can be obtained. It has been reported [159,160] that high strain and high hydrostatic pressure can cause H aggregation. Cao et al. [161] found that the H distribution of 321 stainless steel welded joints in service for six years is concentrated in the phase interface of austenite and ferrite. Fukushima and Birnbaum [162] proved that H was enriched at Ni grain boundaries by the SIMS method, and Oudriss et al. [163] further found that H was enriched at the $\Sigma 3^n$ interface of Ni-based alloys. The SIMS method can detect H distribution information. However, the dissociation degree is not the same for different microstructures. Only intuitive observation of the H distribution makes it difficult to describe H quantitatively.

HMT is a convenient method for detecting the distribution of hydrogen in materials. It can visually detect the hydrogen-enriched locations and the diffusion and escape path of the H atoms. Based on this, researchers can speculate the permeation process of the H atoms, thereby deriving its mechanism and establishing the permeation kinetic model of H atoms. HMT is based on the principle of washing photographic film, and the photosensitive emulsion AgBr or nuclear emulsion is coated on the surface of the specimen to make H with AgBr undergo a redox reaction:

$$Ag^+ + H = Ag + H^+ \quad (5)$$

The Ag elemental particles on the test surface, namely, the position of H, can be observed by TEM to visualize H detection [164]. Momotani et al. [165,166] used HMT to study the effect of the strain rate on the HE of low-carbon martensitic steel during the tensile process and found that H mainly accumulates on dislocations or primary austenite grain boundaries at low strain, resulting in intergranular cracking. In contrast, H does not have enough time to diffuse at high strain, resulting in transgranular cracking. Nagao et al. [167] found that high-strength steel promoted H diffusion when there was bending stress. Many reports [168–172] use HMT to study the enrichment of H at grain boundaries, phase boundaries, inclusions, cracks, and other places under hydrogen or applied stress conditions, which promotes the development of the HE mechanism. HMT can provide the basic characteristics and spatial distribution information of H, but it cannot be quantitatively analyzed. Furthermore, it only shows the final results after diffusion, which cannot reflect the dynamic process of H and cannot obtain the concentration distribution of H.

The small volume and muscular mobility of H atoms have brought challenges to their imaging observation. Furthermore, the solubility of H atoms in steel is very low. Its concentration is usually on the order of ppm, which further increases the difficulty of H observation. The above experimental methods have their advantages and disadvantages, and the combination of different methods can be considered to capture and analyze the hydrogen distribution more accurately. The observation results of hydrogen can be combined with TDA analysis so that the quantitative and qualitative analysis of hydrogen in the metals can be carried out.

Mechanical property measurement

The object of the mechanical property test is the steel specimens with a certain hydrogen content (or in hydrogen-containing condition), and the test aims to study the variation and law of mechanical property parameters of hydrogen-containing steels [173]. The research shows that the performance degradation of steels that leads to HE failure is mainly manifested in the following aspects 1) fracture occurs under conditions far below the yield strength, 2) reduction of tensile ductility, 3) increased fatigue crack growth rate, 4) reduction in fracture toughness, and 5) reduced fatigue life [174–178]. Therefore, test experiments on the mechanical properties of hydrogen-induced degradation are mainly carried out around the above physical quantities.

In the 1980s, Hoover et al. [179] carried out hydrogen-induced deterioration mechanical property tests on a series of high-grade steels with the highest yield strength of 485 MPa (including X65 and X70 steels). The results showed that with the presence of hydrogen, the above steels all showed significant degradation phenomena, such as a decrease in the rate of section shrinkage and tensile strength. When Payer et al. [180] reported the HE problem of low-carbon martensite, it was found that in a hydrogen environment (atmospheric pressure, nonflow environment), the critical fracture stress value σ_c decreased with increasing tensile strength. Later, other reports [181,182] also showed that the hydrogen-induced delayed fracture sensitivity of high-strength steels with tensile strength greater than 1000 MPa increased with increasing strength, and the critical fracture stress σ_c or critical stress intensity factor K_{TH} decreased sharply with increasing strength [183]. It has also been reported that the hydrogen concentration required for HE decreases with increasing pipe strength. For example, Lovicu [184] found that when the material's tensile strength increased from 1200 MPa to 1400 MPa (atmospheric pressure, nonflow environment), HE is hydrogen concentration decreased from 4 wppm to 1 wppm. Nelson et al. [185] also found in an experiment that even in a low-pressure hydrogen environment (0.08 MPa, nonflow environment), when the yield strength of 4130 steel increased from 1050 MPa to 1330 MPa, the critical stress intensity factor K_{TH} decreased from 60 MPa $m^{0.5}$ to approximately 20 MPa $m^{0.5}$, and the HE sensitivity increased significantly.

It can be seen that the above experiments are carried out in a low-pressure environment, the experimental material is a fully hydrogenated metal specimen, but the pressure in practical engineering will be higher. Nanninga and Amaro et al. [22,186,187] obtained high hydrogen pressure (up to 13.8 MPa) using high-pressure vessels and carried out mechanical property experiments in the vessel. The conclusions are as follows 1) in a hydrogen environment, the fatigue crack growth rate of X100 steel increases with increasing hydrogen pressure, and the growth rate increases by 1–2 orders of magnitude compared with that in air, 2) the elongation and section shrinkage of the steel decrease significantly, and 3) when the toughness of the material decreases or the brittleness increases, the crack propagation rate will accelerate. This trend increases with increasing material strength, which further suggests that high-grade steel has higher HE sensitivity.

Thanh et al. [31] analyzed the mechanical properties of X42 pipeline steel by a small punch device in a hydrogen/natural gas mixed environment. Hydrogen-assisted fracture behavior showed a transition from ductile fracture to brittle fracture. In the potential natural test, it was observed that when hydrogen existed in the gas mixture, the fracture of the specimen increased. As shown in Fig. 5(a) and (b), under air and low H_2 partial pressure (0.5%), the test specimen has pitted ductile fracture. When the H_2 partial pressure increases to 1% and the total pressure of the mixed gas reach 7 MPa, the fracture surface of the specimen presents a mixed fracture mode of micro-pore aggregation and quasi-cleavage fracture (Fig. 5 (c)). When the H_2 partial pressure reaches 5%, the fracture surface is entirely characterized by the quasi-cleavage surface's facet structure, and the specimen's lower surface shows a high-density secondary circumferential crack around the main crack (Fig. 5 (d)). When fully exposed to a 100% H_2, 10 MPa environment, the secondary circumferential crack density of the specimen reaches the highest, and the fracture mode shows from ductile fracture to brittle fracture (Fig. 5 (e)). Zhou et al. [30] performed a similar experiment on a universal testing machine with a high-pressure environment cabinet. Nitrogen and natural gas were used to simulate the effect of hydrogen-blended natural gas on the tensile properties of X80 steel. The results show that adding a higher proportion of hydrogen (5% vs 2.2%) significantly increased the impact of tensile strength, elongation after fracture and reduced the area of the notched specimen. The relative tensile strength, elongation after fracture, and relative area reduction are 98.44%, 79.03%, and 86.59%, respectively, indicating that increasing hydrogen results in decreased properties of X80 steel.

In summary, there have been some methods and experimental results for testing the mechanical properties of hydrogenated steels. A high-pressure vessel, a small punch device, and a universal testing machine can test the mechanical properties of steels under high pressure or atmospheric pressure. These experimental results show two basic facts 1) the higher the strength of the pipeline steels, the more significant the mechanical properties deteriorated by hydrogen. 2) the higher the pressure of the test environment and the higher proportion of hydrogen, the more serious the HE of the specimens. However, one issue still needs to be discussed: how does a high proportion of hydrogen exacerbate HE, and whether further addition of hydrogen to the test system will exacerbate HE once the hydrogen content in the metal reaches saturation. This problem may be the work that needs to be solved in the future for mechanical performance testing. One is how to prepare HP experimental specimens that meet the pipeline transportation conditions. The other is how to ensure the stability of environmental pressure and hydrogen content in the mechanical test process to improve the credibility of the experimental results.

Molecular simulation experiments

Since the existing experimental methods cannot provide comprehensive information on hydrogen-degraded pipes, many scholars have used molecular simulations to

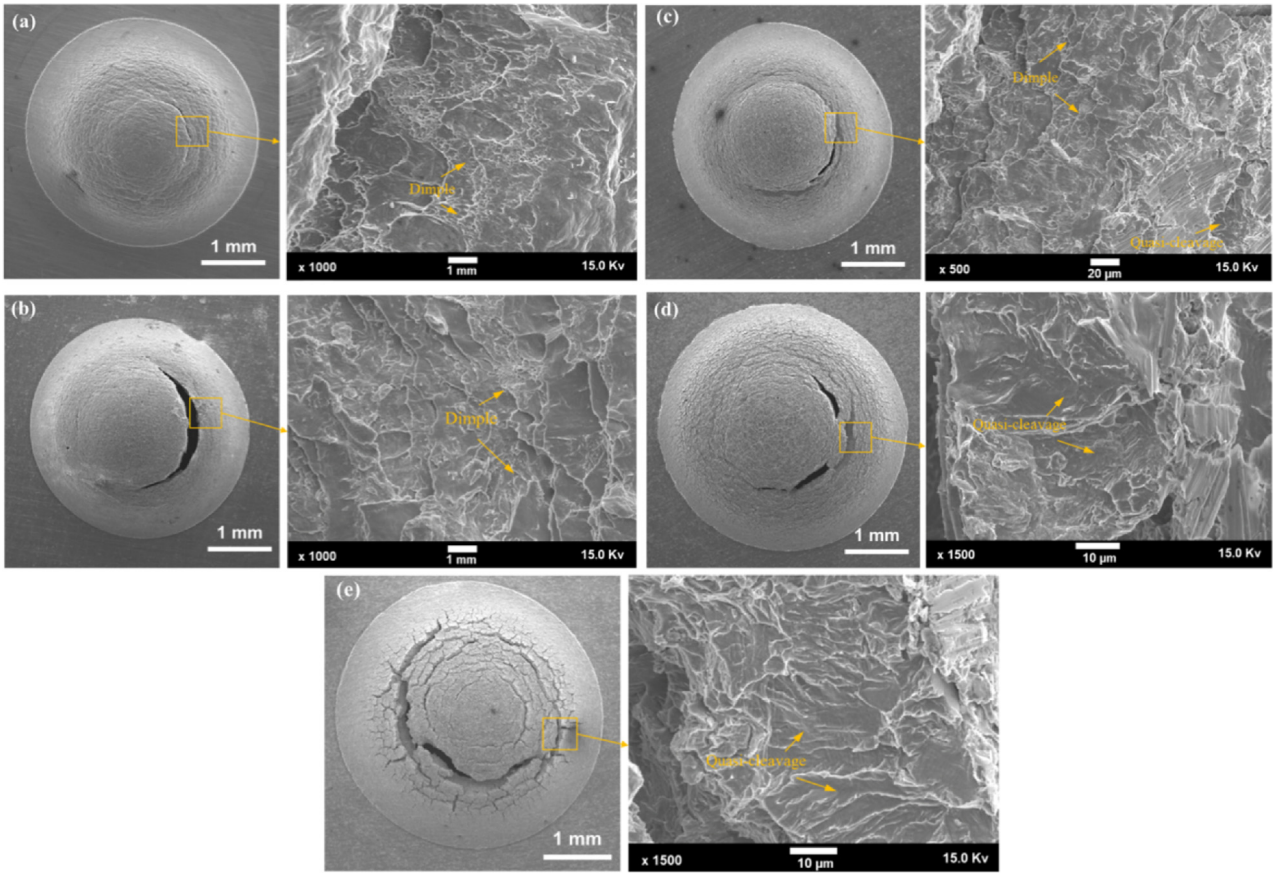

Fig. 5 – —SEM photographs show a higher proportion of hydrogen significantly degrades the metal microstructure: (a) in ambient air, (b) under 7 MPa gas mixture, 0.1% H_2 blend, (c) under 7 MPa gas mixture, 1% H_2 blend, (d) under 7 MPa gas mixture, 5% H_2 blend, and (e) under 10 MPa, 100% H_2 [31].

supplement the relevant experimental data and establish a bridge between theory and experiment in recent years. Molecular dynamics simulation is a multibody simulation method that relies on computers to simulate the movement of molecules and atomic systems and is divided into first-principles molecular dynamics simulations and classical molecular dynamics simulations [188]. The first-principles molecular dynamics simulation calculates the interaction between molecules or atoms based on density functional theory (DFT) [189]. The classical molecular dynamics simulation calculates the potential energy between particles in the system based on empirical evidence of potential or force field. The advantage of classical molecular dynamics simulation is that it runs fast and loads a large model of thousands of atoms for molecular dynamics simulation [190]. Nevertheless, its accuracy depends on the accuracy of the potential empirical function. DFT can accurately describe the interaction between H atoms and metal grain boundaries. However, its calculation speed is slow, the cost is high, and the simulation model generally cannot exceed 100 atoms.

The energy of hydrogen-induced cracking

The energy required for grain boundary cracking is defined as cohesive energy. Yamaguchi et al. [191] calculated the cohesive energy of symmetrical grain boundaries $\sum 3$ (111) of body-centered cubic iron-containing hydrogen by first-principles calculations found that the cohesive energy decreased significantly with increasing H. Gesari et al. [192] also found through molecular simulation that hydrogen segregation at the grain boundary would reduce the Fe–Fe bond energy and the grain boundary cohesion energy, thus leading to the HE of the grain boundary. Wang et al. [193] used the embedded-atom method (EAM) to simulate the interaction between steel and hydrogen under different concentrations of hydrogen. The results show that the cohesive energy of the material decreases by 37% under the action of the hydrogen atom, indicating that the decrease in hydrogen bonding energy is reasonable. Tahir et al. [194] performed similar molecular simulation experiments on carbon steel crystals. The results show that the separation work required to pull the fixed atom away will decrease with increasing hydrogen atom infiltration, which indirectly confirms the HEDE mechanism.

Wang et al. [193] also found through molecular simulation that under hydrogen pressure below 1000 atmospheric pressures, the reduction of reversible separation work of different types of Fe grain boundaries and free surfaces was less than 33%. It increased to 36% under 5000 atmospheric pressures. Near the limit of hydride formation, the reduction rate is 44% at atmospheric pressures of 5×10^4. It is believed that hydrogen-enhanced plasticity and adjoint effects lead to the transformation of the fracture mode, namely, from transgranular fracture to intergranular fracture. Nevertheless,

Solanki et al. [195] calculated the cohesive energy of symmetric grain boundaries with different inclination angles of α-Fe. They found that only part of the cohesive energy of the grain boundary structure was reduced, while the other part of the cohesive energy of the grain boundary structure was increased.

Effect of hydrogen on cracking process

Xu et al. [188] simulated the role of hydrogen in the crack propagation process of single-crystal nickel. They revealed that hydrogen inhibits the embrittlement of plastic deformation during cracking, and with the increase in H atoms at the crack tip, this embrittlement trend is more prominent. Wen et al. [196] simulated a single-crystal iron model containing hydrogen. They found that hydrogen gathered at the crack tip, leading to a severe brittle fracture process, and the results were consistent with the experimental process.

Barrows et al. [197] used statistical methods combined with molecular dynamics simulation to study the effect of hydrogen on intercrystalline exfoliation. The results show that increasing hydrogen coverage at the grain boundaries of Ni crystals will asymmetrically affect the speed of crack tips during crack propagation, resulting in a general decrease in the separation work required for crack propagation and a reduction in the peak stress in the relationship between tensile load and separation. Chandler et al. [198] studied the dimple formation of a face-centered cubic crystal by molecular dynamics simulation and Monte Carlo simulation. They concluded that hydrogen reduced the stress of dimple formation and promoted the appearance of microporous aggregation fracture, which supports the HESIV mechanism. Hu et al. [199] found that hydrogen at the crack tip would promote the expansion and connection of holes in the crack tip region, thereby accelerating the crack propagation through the molecular dynamics simulation of the crack propagation of single-crystal iron at the nanoscale. This conclusion was not consistent with the experimental results of hydrogen-induced embrittlement but was consistent with the HELP theory.

Effect of hydrogen on dislocations

Current reports show that hydrogen has two opposite effects on dislocations: promotion and inhibition.

In terms of inhibition, Xie et al. [200] explained the phenomenon of hydrogen inhibiting dislocation movement in aluminum alloy through a hydrogen-induced vacancy model in molecular simulation and verified this statement through experiments. Through molecular dynamics simulation, Song Jun et al. [115,201] found that the H atoms distributed at the crack tip increased the critical condition for the crack to emit dislocations, which had an inhibitory effect on dislocations further inhibited the generation of plastic deformation.

In terms of the promoting effect, Matsumoto et al. [202] studied the interaction between an edge dislocation and hydrogen in a type I cracked of single-crystal Fe by molecular dynamics simulation and believed that after the dislocation nucleus captured the hydrogen atom, the threshold energy of dislocation movement was reduced so that hydrogen promoted the dislocation movement. Taketomi et al. [203] studied the dislocation emission during the propagation of type II cracks in α-Fe. They believed that the presence of hydrogen reduced the stacking fault energy, thereby promoting the dislocation emission. Lynch [204,205] also used the molecular simulation method to prove that the presence of hydrogen will increase the dislocation density at the grain boundary and form strain, which supports the accuracy of the AIDE mechanism, which is consistent with the results of Adlakha et al. [178] using EAM for molecular dynamics research. Pezold et al. [206] studied the stress shielding effect by a multiscale method combined with DFT and semiempirical EAM potential. They found that the weak hydrogen-hydrogen interaction at the dislocation edge can also significantly reduce the volume concentration of hydrogen, which is necessary to induce the stress shielding effect under the HELP mechanism and provides evidence for the HELP mechanism.

The simulation and calculation results between hydrogen and dislocations show significant differences, and the relationship between hydrogen and dislocations and plastic deformation is controversial at the practical level. Because the simulation simplifies the actual process, the selection of the potential function, the selection of the model, and the cumulative error of calculation will cause differences in simulation results. Although it has been reported that some HE mechanisms have been confirmed by molecular simulation, it is not clear which dominant mechanism is in actual working conditions. The effect of hydrogen on grain boundary cohesive energy and dislocation is also under discussion. Molecular simulation experiments should be used as verification and supplement to the HE mechanisms. However, two problems also need to be solved: 1) why the addition of hydrogen reduces the separation work required to pull the fixed atoms apart, 2) the current reports show that the influence of hydrogen on cohesive energy and dislocations has two sides, molecular simulations can explore the conditions under which these conditions occur, because hydrogen may have two opposite effects on cohesive energy and dislocation under different conditions.

Conclusions and suggestions for further work

This paper discusses the hydrogen-induced failure of high-strength steels, the current experimental methods to study this problem, and the problems and challenges faced by these experimental methods when dealing with high-strength pipeline steels under the condition of high-pressure hydrogen-blended natural gas. The following conclusions and recommendations are obtained:

1) The description of the HE mechanisms is still under discussion and update, and the combination of multiple mechanisms is the technical idea for further research. However, vast amounts of experiments and simulation methods are needed to support it. Further work needs to solve the following problems:
   - The root cause of the interface debonding in the HEDE mechanism. The main driving force of crack propagation in the AIDE mechanism. The reason for the increase or decrease of the dislocation mobility in the HELP mechanism.

- Multi-mechanism synergy needs to ascertain the gradual nature of the HE process and the conditions for stimulating different mechanisms.

2) The commonly used electrochemical hydrogen charging method is no longer applicable for HP experiments because its working condition is not consistent with the actual engineering's. It is necessary to develop new gas-phase hydrogen charging experimental platform. It should include a closed-loop system constructed by high-strength pipelines, valves, compressors, hydrogenation machines, and other equipment. It can provide gas flow conditions and is equipped with precision measuring instruments to obtain accurate data. These data include system operating pressure, hydrogen exposure time, gas flow rate, hydrogen concentration, etc. In this way, researchers can explore the quantitative relationship between the hydrogen dissolved in pipeline steel and these parameters. Then research more practical HE mechanism models and safety assessment methods of pipeline steels.
3) The mechanical property degradation test of steels is based on the HP experiments, so the existing research conclusions must be carefully applied to the safety analysis of natural gas pipe networks with high steel grade and high pressure. The supporting steel mechanical property test experiments should also pay special attention to the stability of the test environment and the reliability of data acquisition. The issues that can be paid attention to in further work are:
   - How does a high proportion of hydrogen aggravate the HE. When the hydrogen content in the metal reaches saturation, whether hydrogen is added to the test system will aggravate the HE.
4) Hydrogen imaging technology cannot capture the trajectory and dynamic process of hydrogen molecules in steels, which limits the interpretation of the microscopic mechanism of HE. The issues that can be paid attention to in further work are:
   - The TDA experiment should analyze the amount of hydrogen infiltration under different experimental parameter levels and infer the relationship between the amount of hydrogen trapped by hydrogen traps with the pressure, exposure time, and hydrogen content, and how the ability of hydrogen traps to trap hydrogen is affected by these parameters impact.
   - The hydrogen distribution observation results can be combined with the TDA experiment to perform a quantitative and qualitative analysis of hydrogen in the metal.
5) The molecular simulation technology of hydrogen-induced degradation of steel performance still has insufficient simulation capabilities and simulation accuracy. Despite some HE mechanisms that have been confirmed by some reports using molecular simulation methods, it has not been concluded which is the dominant mechanism in actual conditions. The influence of hydrogen on cohesive energy of grain boundary and the dislocation is still under discussion. Further research is required to propose new interatomic multiscale models for further simulation that can be used to simulate thousands of atomic systems to reproduce the interaction between hydrogen and grain boundaries during hydrogen-induced fracture and explain the two controversial issues:
   - The influence of hydrogen on the cohesive energy of grain boundary and the dislocation is inhibited or promoted.
   - Why does the addition of hydrogen reduce the separation work required to pull the fixed atoms apart.

Declaration of competing interest

The authors declare that they have no known competing financial interests or personal relationships that could have appeared to influence the work reported in this paper.

Acknowledgment

This paper is supported by the National Natural Science Foundation of China (Programme Grant Number EP/52074238), the Science and Technology Program of Sichuan Province (Programme Grant Number EP/2021YFSY0057), and the Scientific Research Project of the General Administration of Customs of China (Programme Grant Number EP/2019HK076).

REFERENCES

[1] Qadrdan M, Abeysekera M, Wu J, Jenkins N, Winter B. The future of gas networks. Springer; 2020. p. 49–68.
[2] Liakopoulou M. Towards an EU hydrogen economy. Policy; 2020.
[3] Cell F. Road map to a US hydrogen energy: reducing emissions and driving growth across the nation. 2020.
[4] Pluvinage G, Capelle J, Meliani MH. Pipe networks transporting hydrogen pure or blended with natural gas, design and maintenance. Eng Fail Anal 2019;106.
[5] Elaoud S, Hadj-Taïeb E. Transient flow in pipelines of high-pressure hydrogen–natural gas mixtures. Int J Hydrogen Energy 2008;33:4824–32.
[6] Ogden J, Jaffe AM, Scheitrum D, McDonald Z, Miller M. Natural gas as a bridge to hydrogen transportation fuel: insights from the literature. Energy Pol 2018;115:317–29.
[7] Gielen D, Taibi E, Miranda R. Hydrogen: a reviewable energy perspective: report prepared for the 2nd hydrogen energy ministerial meeting in Tokyo. 2019. Japan.
[8] Zhou Z, Ersoy D. Review studies of hydrogen use in natural gas distribution systems. Final Rep GTI Proj 2010;15:2010. 21029, Oct.
[9] Pellegrini M, Guzzini A, Saccani C. A preliminary assessment of the potential of low percentage green hydrogen blending in the Italian natural gas network. Energies 2020;13:5570.
[10] Nagumo M. Fundamentals of hydrogen embrittlement, vol. 921. Springer; 2016.
[11] Whitney G, Behrens CE. Energy: natural gas: the production and use of natural gas, natural gas imports and exports, EPAct project, liquefied natural gas (LNG) import terminals and infrastructure security, underground working gas storage, fischer-tropsch fuels from coal, natural gas, and biomass, gas hydrates, gas shales, hydraulic fracturing, Alaska natural gas pipelines. The Capitol Net Inc; 2009.

[12] Yin Y, Huang Y, Yao Y, et al. The development of X80 steel plate and coil for the 2nd west-east pipeline project[C]. In: International Pipeline Conference; 2008. p. 147–55.
[13] Feng Y-r, Zhuang C-j. Application problems of grade X80 pipeline project [J]. Welded Pipe and Tube 2006;1.
[14] Ma Q, Huo C. Comparison and analysis on specification of X80 line pipe for 2nd West-east Gas Transmission Pipeline Project[C]. International Pipeline Conference. 2010. p. 699–705.
[15] Zhang J, Zheng H, He W, Huang W. West-east gas pipeline project. Frontiers of Engineering Management 2020;7:163–7.
[16] SuiGirth Y. Welding on oil and gas pipeline projects in China[C]. In: Chinese Materials Conference; 2017. p. 1143–54.
[17] Fischer S. Nord Stream 2: trust in Europe. CSS Policy Perspectives 2016;4.
[18] Minato I, Takahashi N, Nishi Y. Successful production results of SAWL 485 I FD (X70) UOE pipes for NORD STREAM [C]. In: The Twenty-second International Offshore and Polar Engineering Conference; 2012.
[19] Han YD, Wang RZ, Wang H, Xu LY. Hydrogen embrittlement sensitivity of X100 pipeline steel under different pre-strain. Int J Hydrogen Energy 2019;44.
[20] Al-Mansour M, Alfantazi A, El-Boujdaini M. Sulfide stress cracking resistance of API-X100 high strength low alloy steel. Mater Des 2009;30:4088–94.
[21] Dong C, Liu Z, Li X, Cheng Y. Effects of hydrogen-charging on the susceptibility of X100 pipeline steel to hydrogen-induced cracking. Int J Hydrogen Energy 2009;34:9879–84.
[22] Nanninga N, et al. Comparison of hydrogen embrittlement in three pipeline steels in high pressure gaseous hydrogen environments. Corrosion Sci 2012;59:1–9.
[23] Cauwels M, Claeys L, Depover T, Verbeken K. The hydrogen embrittlement sensitivity of duplex stainless steel with different phase fractions evaluated by in-situ mechanical testing. Frat Ed Integrità Strutt 2020:449–58.
[24] Capelle J, Gilgert J, Dmytrakh I, Pluvinage G. Sensitivity of pipelines with steel API X52 to hydrogen embrittlement. Int J Hydrogen Energy 2008;33:7630–41.
[25] Yamabe J, Yoshikawa M, Matsunaga H, Matsuoka S. Effects of hydrogen pressure, test frequency and test temperature on fatigue crack growth properties of low-carbon steel in gaseous hydrogen. In: 21st European Conference on Fracture, 2; 2016. p. 525–32. https://doi.org/10.1016/j.prostr.2016.06.068. Ecf21.
[26] Loginow A, Phelps E. Steels for seamless hydrogen pressure vessels. Corrosion 1975;31:404–12.
[27] Johnson WH. On some remarkable changes produced in iron and steel by the action of hydrogen and acids. Nature 1875;11:393.
[28] Alen T, S JA. Effect of cold-rolling on hydrogen diffusion and trapping in X70 pipeline steel. J Eng Mater Technol 2021;143.
[29] Zhang T, et al. Comparison of hydrogen embrittlement susceptibility of three cathodic protected subsea pipeline steels from a point of view of hydrogen permeation. Corrosion Sci 2018;131.
[30] Dengji Z, et al. The experiment study to assess the impact of hydrogen blended natural gas on the tensile properties and damage mechanism of X80 pipeline steel. Int J Hydrogen Energy 2020;46(10):7402–14.
[31] Thanh TN, Jong SP, Seung HN, Un BB. Evaluation of hydrogen related degradation of API X42 pipeline under hydrogen/natural gas mixture conditions using small punch test. Theor Appl Fract Mech 2021;133:10296.
[32] Mohtadi-Bonab M, Szpunar J, Razavi-Tousi S. A comparative study of hydrogen induced cracking behavior in API 5L X60 and X70 pipeline steels. Eng Fail Anal 2013;33:163–75.
[33] Takahashi J, Kawakami K, Tarui T. Direct observation of hydrogen-trapping sites in vanadium carbide precipitation steel by atom probe tomography. Scripta Mater 2012;67.
[34] Takahashi J, Kawakami K, Kobayashi Y. Origin of hydrogen trapping site in vanadium carbide precipitation strengthening steel. Acta Mater 2018;153:193–204.
[35] Takahashi J, Kawakami K, Kobayashi Y, Tarui T. The first direct observation of hydrogen trapping sites in TiC precipitation-hardening steel through atom probe tomography. Scripta Mater 2010;63:261–4.
[36] Rivarolo M, Marmi S, Riveros-Godoy G, Magistri L. Development and assessment of a distribution network of hydro-methane, methanol, oxygen and carbon dioxide in Paraguay. Energy Convers Manag 2014;77:680–9. https://doi.org/10.1016/j.enconman.2013.09.062.
[37] Stiller C, et al. Pathways to a hydrogen fuel infrastructure in Norway. Int J Hydrogen Energy 2009;35.
[38] Messaoudani Zl, Rigas F, Hamid MDB, Hassan CRC. Hazards, safety and knowledge gaps on hydrogen transmission via natural gas grid: a critical review. Int J Hydrogen Energy 2016;41.
[39] Ozturk M, Dincer I. A comprehensive review on power-to-gas with hydrogen options for cleaner applications. Int J Hydrogen Energy 2021;46(62):31511–2.
[40] Zschocke A. Pilotanlage windgas falkenhagen. Aqua Gas 2015;95.
[41] Judd R, Pinchbeck D. Compendium of hydrogen energy. Elsevier; 2016. p. 165–92.
[42] Bourne S. The future of fuel: the future of hydrogen. Fuel Cell Bull 2012;2012:12–5.
[43] Pimm AJ, Yang J, Widjaja K, Cockerill TT. Hydrogen technology state of the art. 2019.
[44] Mauberger C. GDF Suez, McPhy in French GRHYD project on methane, hydrogen. Fuel Cell Bull 2012.
[45] Gaz RDF-G, Engie I, GNVert-Engie F, McPhy EF. GRHYD-Management of Networks by injection of Hydrogen to De-carbonate energies. Press file. The GRHYD project partners inaugurate the first Power-to-Gas demonstrator in France. 2018.
[46] Kungl G. The incumbent German power companies in a changing environment: a comparison of E. ON, RWE, EnBW and Vattenfall from 1998 to 2013. Discussion Paper. SOI; 2014.
[47] Iskov H, Rasmussen NB. Global screening of projects and technologies for Power-to-Gas and Bio-SNG. A reference report. Horsholm: Danish Gas Technology Centre; 2013.
[48] Wacket M. Germany to phase out coal by 2038 in move away from fossil fuels. Thomson Reuters; 2019.
[49] Kopp M, et al. Energiepark Mainz: technical and economic analysis of the worldwide largest Power-to-Gas plant with PEM electrolysis. Int J Hydrogen Energy 2017;42:13311–20.
[50] Saba SM, Müller M, Robinius M, Stolten D. The investment costs of electrolysis–A comparison of cost studies from the past 30 years. Int J Hydrogen Energy 2018;43:1209–23.
[51] Motalebi S, Barnes T, Kaspar S, Niet T, Wright AS. Hydrogen to provide flexibility in the Canadian energy system. 2021.
[52] Stansberry JM, Brouwer J. Experimental dynamic dispatch of a 60 kW proton exchange membrane electrolyzer in power-to-gas application. Int J Hydrogen Energy 2020;45:9305–16.
[53] Isaac T. HyDeploy: the UK's first hydrogen blending deployment project. Clean Energy 2019;3:114–25.
[54] Scott M, Powells G. Blended hydrogen: the UK public's perspective. 2019.
[55] Fairley P. Germany's green-energy gap. IEEE Spectrum 2009;46:40–8.
[56] Meißner AC, et al. 16th international conference on the European energy market (EEM). IEEE; 2019. p. 1–6.

[57] Karolytė R. Hydrogen with CCS for decarbonised heat in the Scottish context. 2017.
[58] Analytica O. Pipeline to Italy will change Balkan energy market. Emerald Expert Briefings 2021;54(9):22–3.
[59] Alverà M. The Italian utilities industry. Springer; 2020. p. 227–41.
[60] Florisson O. Preparing for the hydrogen economy by using the existing natural gas system as a catalyst. NaturalHy Project Rep SES6 2010:502661.
[61] Tiekstra G, Koopman F. The NaturalHy Project: first step in assessing the potential of existing natural gas network for hydrogen delivery[C]. International Gas Union Research Conference. Paris. 2008.
[62] Melaina MW, Antonia O, Penev M. Blending hydrogen into natural gas pipeline networks: a review of key issues. 2013.
[63] Ehrhart BD, Hecht E, Muna AB, LaFleur CB. Hydrogen risk assessment models 2.0: open-source quantitative risk assessment framework. Albuquerque, NM (United States); Sandia: Sandia National Lab.(SNL-NM); 2020.
[64] Roadmap E. National hydrogen energy roadmap. US department of energy (DOE). Washington, DC: National Hydrogen Energy Roadmap; 2002 (2002).
[65] Ruf Y, Lange S, Droege C, Pfister J. Fuel cells and hydrogen for green energy in European cities and regions. 2018.
[66] Kaiser MJ. The global offshore pipeline construction service market 2017 – Part I. Ships Offshore Struct 2018;13.
[67] Reed M. Global pipeline construction outlook 2021. Pipeline Gas J 2021;248.
[68] Khalid HU, Ismail MC, Nosbi N. Permeation damage of polymer liner in oil and gas pipelines: a review. Polym Bull 2020;12:2307.
[69] Tubb R. P&GJ's 2017 worldwide pipeline construction report. Pipeline Gas J 2017;244:16–20.
[70] Asadipoor M, Anaraki AP, Kadkhodapour J, Sharifi SMH, Barnoush A. Macro- and microscale investigations of hydrogen embrittlement in X70 pipeline steel by in-situ and ex-situ hydrogen charging tensile tests and in-situ electrochemical micro-cantilever bending test. Mater Sci Eng, A 2020;772.
[71] Neeraj T, Srinivasan R, Li J. Hydrogen embrittlement of ferritic steels: observations on deformation microstructure, nanoscale dimples and failure by nanovoiding. Acta Mater 2012;60.
[72] Bai P-p, et al. Hydrogen embrittlement of X80 pipeline steel in H_2S environment: effect of hydrogen charging time, hydrogen-trapped state and hydrogen charging–releasing–recharging cycles. International Journal of Minerals Metallurgy and Materials 2020;27:63–73.
[73] Qi Y, et al. Comparison of tensile and impact behavior of carbon steel in H 2 S environments. Mater Des 2014;58.
[74] Xue HB, Cheng YF. Characterization of inclusions of X80 pipeline steel and its correlation with hydrogen-induced cracking. Corrosion Sci 2010;53.
[75] Pundt A, Kirchheim R. Hydrogen in metals: microstructural aspects. Annu Rev Mater Res 2006;36:555–608.
[76] Martínez-Pañeda E, Niordson CF, Gangloff RP. Strain gradient plasticity-based modeling of hydrogen environment assisted cracking. Acta Mater 2016;117:321–32.
[77] Mohtadi-Bonab M, Szpunar J, Basu R, Eskandari M. The mechanism of failure by hydrogen induced cracking in an acidic environment for API 5L X70 pipeline steel. Int J Hydrogen Energy 2015;40:1096–107.
[78] Ahn D, Sofronis P, Dodds Jr R. On hydrogen-induced plastic flow localization during void growth and coalescence. Int J Hydrogen Energy 2007;32:3734–42.
[79] Neeraj T, Srinivasan R, Li J. Hydrogen embrittlement of ferritic steels: observations on deformation microstructure, nanoscale dimples and failure by nanovoiding. Acta Mater 2012;60:5160–71.
[80] Zhang S, et al. Investigating the influence mechanism of hydrogen partial pressure on fracture toughness and fatigue life by in-situ hydrogen permeation. Int J Hydrogen Energy 2021;46:20621–9.
[81] Hejazi D, et al. Effect of manganese content and microstructure on the susceptibility of X70 pipeline steel to hydrogen cracking. Mater Sci Eng, A 2012;551.
[82] Kim WK, Koh SU, Yang BY, Kim KY. Effect of environmental and metallurgical factors on hydrogen induced cracking of HSLA steels. Corrosion Sci 2008;50.
[83] Sun B, et al. Current challenges and opportunities toward understanding hydrogen embrittlement mechanisms in advanced high-strength steels: a review. Acta Metall Sin 2021:1–14.
[84] Zapffe C, Sims C. Hydrogen embrittlement, internal stress and defects in steel. Trans. AIME 1941;145:225–71.
[85] Sezgin J-G, Bosch C, Montouchet A, Perrin G, Wolski K. Modelling of hydrogen induced pressurization of internal cavities. Int J Hydrogen Energy 2017;42.
[86] Bae D-S, et al. Effect of highly pressurized hydrogen gas charging on the hydrogen embrittlement of API X70 steel. Met Mater Int 2014;20.
[87] Sezgin J-G, Yamabe J. Simulation of the impact of internal pressure on the integrity of a hydrogen-charged Type-316L stainless steel during slow strain rate tensile test. Int J Hydrogen Energy 2018;43.
[88] Pfeil LB. The effect of occluded hydrogen on the tensile strength of iron. Proc R Soc Lond - Ser A Contain Pap a Math Phys Character 1926;112:182–95.
[89] Gerberich WW, Oriani RA, Lji M-J, Chen X, Foecke T. The necessity of both plasticity and brittleness in the fracture thresholds of iron. Philos Mag A 1991;63:363–76.
[90] Dear FF, Skinner GCG. Mechanisms of hydrogen embrittlement in steels: discussion. Phil Trans 2017;375:20170032.
[91] Bitzek E, Kermode JR, Gumbsch P. Atomistic aspects of fracture. Int J Fract 2015;191.
[92] Daw MS, Baskes MI. Application of the embedded atom method to hydrogen embrittlement. Chemistry and Physics of Fracture 1987;130:196–218.
[93] Jokl ML, Vitek V, McMahon CJ. A microscopic theory of brittle fracture in deformable solids: a relation between ideal work to fracture and plastic work. Acta Metall 1980;28.
[94] Oriani RA. Hydrogen—the versatile embrittler. Corrosion 1987;43:390–7.
[95] Sun B, et al. Current challenges and opportunities toward understanding hydrogen embrittlement mechanisms in advanced high-strength steels: a review. Acta Metall Sin 2021:1–14 (English Letters).
[96] Barrera O, et al. Understanding and mitigating hydrogen embrittlement of steels: a review of experimental, modelling and design progress from atomistic to continuum. J Mater Sci 2018;53:6251–90.
[97] Troiano AR. The role of hydrogen and other interstitials in the mechanical behavior of metals. Metallogr Microstruct Anal 2016;5:557–69.
[98] Beachem CD. A new model for hydrogen-assisted cracking (hydrogen "embrittlement"). Metall Mater Trans B 1972;3:441–55.
[99] Lynch SP. Hydrogen embrittlement and liquid-metal embrittlement in nickel single crystals. Scripta Metall 1979;13:1051–6.
[100] Marcus P. Corrosion mechanisms in theory and practice. CRC press; 2011.
[101] Christmann K. Interaction of hydrogen with solid surfaces. Surf Sci Rep 1988;9:1–163.

[102] Christmann K. Some general aspects of hydrogen chemisorption on metal surfaces. Prog Surf Sci 1995;48:15–26.
[103] Shih DS, Robertson IM, Birnbaum HK. Hydrogen embrittlement of α titanium: in situ tem studies. Acta Metallurgica 1988;36:111–24.
[104] Birnbaum HK, Sofronis P. Hydrogen-enhanced localized plasticity—a mechanism for hydrogen-related fracture. Mater Sci Eng, A 1994;176:191–202.
[105] Shan D, Zong Y, Lv Y, Guo B. The effect of hydrogen on the strengthening and softening of Ti–6Al–4V alloy. Scripta Mater 2008;58:449–52.
[106] Lynch S. Environmentally assisted cracking: overview of evidence for an adsorption-induced localised-slip process. Acta Metall 1988;36:2639–61.
[107] Lynch SP. 9 – metallographic and fractographic techniques for characterising and understanding hydrogen-assisted cracking of metals. Gaseous Hydrogen Embrittlement of Materials in Energy Technologies 2012:63–104.
[108] Nagumo M. Function of hydrogen in embrittlement of high-strength steels. ISIJ Int 2001;41:590–8.
[109] Nagumo M. Hydrogen related failure of steels – a new aspect. Metal Science Journal 2004;20:940–50.
[110] Hickel T, et al. Ab InitioBased understanding of the segregation and diffusion mechanisms of hydrogen in steels. J Occup Med 2014;66:1399–405.
[111] Sakaki K, et al. The effect of hydrogen on vacancy generation in iron by plastic deformation. Scripta Mater 2006;55:1031–4.
[112] Neeraj T, Srinivasan R, Li J. Hydrogen embrittlement of ferritic steels: observations on deformation microstructure, nanoscale dimples and failure by nanovoiding. Acta Mater 2012;60:5160–71.
[113] Fu L, Fang H. Atomistic investigation of hydrogen embrittlement effect for symmetric and asymmetric grain boundary structures of bcc Fe. Comput Mater Sci 2019;158:58–64.
[114] Fu L, Fang H. Formation criterion of hydrogen-induced cracking in steel based on fracture mechanics. Metals-Basel 2018;8:940.
[115] Song J, Curtin W. Atomic mechanism and prediction of hydrogen embrittlement in iron. Nat Mater 2013;12:145–51.
[116] Martin ML, Dadfarnia M, Nagao A, Wang S, Sofronis P. Enumeration of the hydrogen-enhanced localized plasticity mechanism for hydrogen embrittlement in structural materials. Acta Mater 2018;165.
[117] Shuang L, Minsheng H, Lv Z, Yaxin Z, Zhenhuan L. Effect of multiple hydrogen embrittlement mechanisms on crack propagation behavior of FCC metals: competition vs. synergy. Int J Plast 2021;143:103023.
[118] Devanathan MAV, Stachurski Z. The adsorption and diffusion of electrolytic hydrogen in palladium. Proc Roy Soc Lond Math Phys Sci 1962;270:1934–90.
[119] Thomas KF, Davis MJ, Kheruntsyan KV. Thermalization of a quantum Newton's cradle in a one-dimensional quasicondensate. Phys Rev A 2021;103:023315.
[120] Choo WY. Effect of cathodic charging current density on the apparent hydrogen diffusivity through pure iron. J Mater Sci 1984;19.
[121] Archer MD, Grant NC. Achievable boundary conditions in potentiostatic and galvanostatic hydrogen permeation through palladium and nickel foils. Proc Roy Soc Lond Math Phys Sci 1984;395:1934–90.
[122] Thomas A, Szpunar JA. Hydrogen diffusion and trapping in X70 pipeline steel. Int J Hydrogen Energy 2020;45.
[123] Akiyama E, Li S. Electrochemical hydrogen permeation tests under galvanostatic hydrogen charging conditions conventionally used for hydrogen embrittlement study. Corrosion Rev 2016;34:103–12.
[124] Asadipoor M, Anaraki AP, Kadkhodapour J, Sharifi S, Barnoush A. Macro-and microscale investigations of hydrogen embrittlement in X70 pipeline steel by in-situ and ex-situ hydrogen charging tensile tests and in-situ electrochemical micro-cantilever bending test. Mater Sci Eng, A 2020;772:138762.
[125] Zhang T, et al. Comparison of hydrogen embrittlement susceptibility of three cathodic protected subsea pipeline steels from a point of view of hydrogen permeation. Corrosion Sci 2018;131:104–15.
[126] Zhang TM, et al. Comparison of hydrogen embrittlement susceptibility of three cathodic protected subsea pipeline steels from a point of view of hydrogen permeation. Corrosion Sci 2018;131:104–15. https://doi.org/10.1016/j.corsci.2017.11.013.
[127] Zhao W, Zhang T, He Z, Sun J, Wang Y. Determination of the critical plastic strain-induced stress of X80 steel through an electrochemical hydrogen permeation method. Electrochim Acta 2016;214.
[128] Zhao WM, Zhang TM, Zhao YJ, Sun JB, Wang Y. Hydrogen permeation and embrittlement susceptibility of X80 welded joint under high-pressure coal gas environment. Corrosion Sci 2016;111:84–97. https://doi.org/10.1016/j.corsci.2016.04.029.
[129] Shuai Z, et al. Investigating the influence mechanism of hydrogen partial pressure on fracture toughness and fatigue life by in-situ hydrogen permeation. Int J Hydrogen Energy 2021;46.
[130] Choo WY, Lee JY. Thermal analysis of trapped hydrogen in pure iron. Metall Trans A 1982;13.
[131] Takai K, Homma Y, Izutsu K, Nagumo M. Identification of trapping sites in high-strength steels by secondary ion mass spectrometry for thermally desorbed hydrogen. Nippon Kinzoku Gakkaishi 1996;60:1155–62 (1952).
[132] Hagi H, Hayashi Y. Effect of dislocation trapping on hydrogen and deuterium diffusion in iron. Transactions of the Japan institute of metals 1987;28:368–74.
[133] Kumnick A, Johnson H. Deep trapping states for hydrogen in deformed iron. Acta Metall 1980;28:33–9.
[134] Han J, Nam J-H, Lee Y-K. The mechanism of hydrogen embrittlement in intercritically annealed medium Mn TRIP steel. Acta Mater 2016;113:1–10.
[135] Itoh G, Haramura N, Ihara T. Behavior of hydrogen in an Ni3Al compound investigated by means of hydrogen microprint technique. Nippon Kinzoku Gakkaishi 1999;63:593–6 (1952).
[136] Takai K, Watanuki R. Hydrogen in trapping states innocuous to environmental degradation of high-strength steels. ISIJ Int 2003;43:520–6.
[137] Lee H, Lee J-Y. Hydrogen trapping by TiC particles in iron. Acta Metall 1984;32:131–6.
[138] Jia W, Yang F, Wu X, Li C, Wang Y. Predictions on temperatures of high-pressure gas/water/MEG mixtures flowing through wellhead chokes. J Nat Gas Sci Eng 2020;74.
[139] Wenlong J, Fan Y, Changjun L, Ting H, Shuoshuo S. A unified thermodynamic framework to compute the hydrate formation conditions of acidic gas/water/alcohol/electrolyte mixtures up to 186.2 MPa. Energy 2021;230.
[140] Saito K, Hirade T, Takai K. Hydrogen desorption spectra from excess vacancy-type defects enhanced by hydrogen in tempered martensitic steel showing quasi-cleavage fracture. Metall Mater Trans 2019;50:5091–102.
[141] Ono K, Meshii M. Hydrogen detrapping from grain boundaries and dislocations in high purity iron. Acta Metall Mater 1992;40:1357–64.

[142] Wei F, Hara T, Tsuzaki K. Precise determination of the activation energy for desorption of hydrogen in two Ti-added steels by a single thermal-desorption spectrum. Metall Mater Trans B 2004;35:587–97.
[143] Evers S, Rohwerder M. The hydrogen electrode in the "dry": a Kelvin probe approach to measuring hydrogen in metals. Electrochem Commun 2012;24:85–8.
[144] Robertson IM, et al. Hydrogen embrittlement understood. Metall Mater Trans B 2015;46:1085–103.
[145] Evers S, Senöz C, Rohwerder M. Hydrogen detection in metals: a review and introduction of a Kelvin probe approach. Sci Technol Adv Mater 2013;14(1):014201.
[146] Perez T, Garcia JO. Direct observation of hydrogen evolution in the electron microscope scale. Scripta Metall 1982;16:161–4.
[147] Kelly TF, Larson DJ. The second revolution in atom probe tomography. MRS Bull 2012;37.
[148] Piller J, Haasen P. View Correspondence. Atom probe field ion microscopy of a FeNiB glass. Acta Metall 1982;30:1–8. https://doi.org/10.1016/0001-6160(82)90038-4.
[149] Kolli RP. Atom probe tomography: a review of correlative analysis of interfaces and precipitates in metals and alloys. J Occup Med: J Miner Met Mater Soc 2018;70:1725–35. https://doi.org/10.1007/s11837-018-2934-9.
[150] Miller M. Atom probe field ion microscopy. Vacuum 1994;45:819–31. https://doi.org/10.1016/0042-207x(94)90117-1.
[151] Müller EW. Advances in atom-probe field ion microscopy. J Microsc 1974;100:121–31. https://doi.org/10.1111/j.1365-2818.1974.tb03922.x.
[152] Jiang YF, et al. Atom probe tomographic observation of hydrogen trapping at carbides/ferrite interfaces for a high strength steel. J Mater Sci Technol 2018;34:1344–8.
[153] Fan YH, et al. The role of reversed austenite in hydrogen embrittlement fracture of S41500 martensitic stainless steel. Acta Mater 2017;139.
[154] Crewe A, Wall J. Contrast in a high resolution scanning transmission electron microscope. Optik 1970;30:461–74.
[155] Meyer JC, Girit CO, Crommie MF, Zettl A. Imaging and dynamics of light atoms and molecules on graphene. Nature: International weekly journal of science 2008;454.
[156] Wang G, Yan Y, Yang X, Li J, Qiao L. Investigation of hydrogen evolution and enrichment by scanning Kelvin probe force microscopy. Electrochem Commun 2013;35.
[157] Li M, Guo LQ, Qiao LJ, Bai Y. The mechanism of hydrogen-induced pitting corrosion in duplex stainless steel studied by SKPFM. Corrosion Sci 2012;60.
[158] Guo LQ, et al. Effect of hydrogen on pitting susceptibility of 2507 duplex stainless steel. Corrosion Sci 2013;70.
[159] Yu G-H, et al. Hydrogen accumulation and hydrogen-induced cracking of API C90 tubular steel. Corrosion 1997;53.
[160] Mao SX, Li M. Mechanics and thermodynamics on the stress and hydrogen interaction in crack tip stress corrosion: experiment and theory. J Mech Phys Solid 1998;46:1125–37.
[161] Cao R, et al. Coupling effect of microstructure and hydrogen absorbed during service on pitting corrosion of 321 austenitic stainless steel weld joints. Corrosion Sci 2020;164.
[162] Fukushima H, Birnbaum H. Perspectives in hydrogen in metals. Elsevier; 1986. p. 437–45.
[163] Oudriss A, et al. Meso-scale anisotropic hydrogen segregation near grain-boundaries in polycrystalline nickel characterized by EBSD/SIMS. Mater Lett 2016;165:217–22.
[164] Ovejero-García J. Hydrogen microprint technique in the study of hydrogen in steels. J Mater Sci 1985;20:2623–9.
[165] Momotani Y, Shibata A, Terada D, Tsuji N. Hydrogen embrittlement behavior at different strain rates in low-carbon martensitic steel. Mater Today Proc 2015;2:S735–8.
[166] Momotani Y, Shibata A, Terada D, Tsuji N. Effect of strain rate on hydrogen embrittlement in low-carbon martensitic steel. Int J Hydrogen Energy 2017;42:3371–9.
[167] Nagao A, Kuramoto S, Ichitani K, Kanno M. Visualization of hydrogen transport in high strength steels affected by stress fields and hydrogen trapping. Scripta Mater 2001;45:1227–32.
[168] Chen S, Wu T, Wu. J. Effects of deformation on hydrogen degradation in a duplex stainless steel. J Mater Sci 2004;39:67–71.
[169] Pu S, Turk A, Lenka S, Ooi S. Study of hydrogen release resulting from the transformation of austenite into martensite. Mater Sci Eng, A 2019;754:628–35.
[170] Yoshioka M, Ueno A, Kishimoto H. Analysis of hydrogen behaviour in crack growth tests of γ-TiAl by means of the hydrogen microprint technique. Intermetallics 2004;12:23–31.
[171] Matsunaga H, Noda H. Visualization of hydrogen diffusion in a hydrogen-enhanced fatigue crack growth in type 304 stainless steel. Metall Mater Trans 2011;42:2696–705.
[172] Itoh G, Haramura N, Ihara T. Behavior of hydrogen in an Ni3Al compound investigated by means of hydrogen microprint technique. Intermetallics 2000;8:599–603.
[173] Barrera O, Bombac D, Chen Y, Daff TD, Galindo-Nava E. Understanding and mitigating hydrogen embrittlement of steels: a review of experimental, modelling and design progress from atomistic to continuum. J Mater Sci 2018;53:6251–90.
[174] Horikawa K, Ando N, Kobayashi H, Urushihara W. Visualization of hydrogen gas evolution during deformation and fracture in SCM 440 steel with different tempering conditions. Mater Sci Eng, A 2012;534.
[175] Matsunaga H, Yoshikawa M, Kondo R, Yamabe J, Matsuoka S. Slow strain rate tensile and fatigue properties of Cr–Mo and carbon steels in a 115 MPa hydrogen gas atmosphere. Int J Hydrogen Energy 2015;40.
[176] Wang R. Effects of hydrogen on the fracture toughness of a X70 pipeline steel. Corrosion Sci 2009;51.
[177] Lynch S. Discussion of some recent literature on hydrogen-embrittlement mechanisms: addressing common misunderstandings. Corrosion Rev 2019;37:377–96.
[178] Adlakha I, Solanki K. Critical assessment of hydrogen effects on the slip transmission across grain boundaries in α-Fe. Proc Math Phys Eng Sci 2016;472:20150617.
[179] Hoover WR, Robinson SL, Stoltz RE, Spingarn JR. Hydrogen compatibility of structural materials for energy storage and transmission. Final report. 1981.
[180] Payer J, Preban A, Leckie H. Hydrogen-stress cracking of low-carbon martensitic steel. Corrosion 1976;32:52–6.
[181] Ding YSa, Tsay LWa, Chiang MFb, Chen Cb. Gaseous hydrogen embrittlement of PH 13-8 Mo steel. J Nucl Mater 2009;385:538–44. https://doi.org/10.1016/j.jnucmat.2008.12.048.
[182] Komatsuzaki Y, Joo H, Yamada K. Influence of yield strength levels on crack growth mode in delayed fracture of structural steels. Eng Fract Mech 2008;75:551–9. https://doi.org/10.1016/j.engfracmech.2007.02.009.
[183] Wang G, et al. Hydrogen embrittlement assessment of ultra-high strength steel 30CrMnSiNi2. Corrosion Sci 2013;77:273–80. https://doi.org/10.1016/j.corsci.2013.08.013.
[184] Lovicu G, et al. Hydrogen embrittlement of automotive advanced high-strength steels. Metall Mater Trans 2012;43:4075–87.
[185] Nelson HG, Williams D. Quantitative observations of hydrogen-induced, slow crack growth in a low alloy steel. Stress corrosion cracking and hydrogen embrittlement of iron base alloys. 1977. p. 390–404.

[186] Amaro RL, Drexler ES, Slifka AJ. Fatigue crack growth modeling of pipeline steels in high pressure gaseous hydrogen. Int J Fatig 2014;62:249–57.
[187] Drexler ES, et al. Fatigue crack growth rates of API X70 pipeline steel in a pressurized hydrogen gas environment. Fatig Fract Eng Mater Struct 2014;37.
[188] Xu X, Wen M, Hu Z, Fukuyama S, Yokogawa K. Atomistic process on hydrogen embrittlement of a single crystal of nickel by the embedded atom method. Comput Mater Sci 2002;23.
[189] Dreizler Reiner M, Gross Eberhard KU. Density functional theory. Berlin, Heidelberg: Springer; 2013.
[190] Li J, Lu C, Pei L, Zhang C, Wang R. Atomistic investigation of hydrogen induced decohesion of Ni grain boundaries. Mech Mater 2020;150.
[191] Yamaguchi M. First-principles study on the grain boundary embrittlement of metals by solute segregation: Part I. iron (Fe)-solute (B, C, P, and S) systems. Metall Mater Trans 2011;42:319–29.
[192] Gesari S, Pronsato M, Juan A. The electronic structure and bonding of H pairs at Σ= 5 BCC Fe grain boundary. Appl Surf Sci 2002;187:207–17.
[193] Wang S, Martin ML, Robertson IM, Sofronis P. Effect of hydrogen environment on the separation of Fe grain boundaries. Acta Mater 2016;107:279–88.
[194] Tahir A, Janisch R, Hartmaier A. Hydrogen embrittlement of a carbon segregated Σ5 (310)[001] symmetrical tilt grain boundary in α-Fe. Mater Sci Eng, A 2014;612:462–7.
[195] Solanki KN, Tschopp MA, Bhatia MA, Rhodes NR. Atomistic investigation of the role of grain boundary structure on hydrogen segregation and embrittlement in α-Fe. Metall Mater Trans 2013;44:1365–75.
[196] Wen M, Xu X, Fukuyama S, Yokogawa K. Embedded-atom-method functions for the body-centered-cubic iron and hydrogen. J Mater Res 2001;16:3496–502. https://doi.org/10.1557/jmr.2001.0480.
[197] Barrows W, Dingreville R, Spearot D. Traction–separation relationships for hydrogen induced grain boundary embrittlement in nickel via molecular dynamics simulations. Mater Sci Eng, A 2016;650.
[198] Chandler MQ, et al. Hydrogen effects on nanovoid nucleation in face-centered cubic single-crystals. Acta Mater 2008;56:95–104.
[199] Hu Z, Fukuyama S, Yokogawa K, Okamoto S. Hydrogen embrittlement of a single crystal of iron on a nanometre scale at a crack tip by molecular dynamics. Model Simulat Mater Sci Eng 1999;7:541.
[200] Xie D, et al. Hydrogenated vacancies lock dislocations in aluminium. Nat Commun 2016;7:1–7.
[201] Song J, Soare M, Curtin W. Testing continuum concepts for hydrogen embrittlement in metals using atomistics. Model Simulat Mater Sci Eng 2010;18:045003.
[202] Matsumoto R, Taketomi S, Matsumoto S, Miyazaki N. Atomistic simulations of hydrogen embrittlement. Int J Hydrogen Energy 2009;34.
[203] Taketomi S, Matsumoto R, Miyazaki N. Atomistic study of the effect of hydrogen on dislocation emission from a mode II crack tip in alpha iron. Int J Mech Sci 2010;52:334–8.
[204] Lynch S. Understanding mechanisms and kinetics of environmentally assisted cracking. BHM Berg-und Hüttenmännische Monatshefte 2016;161:3–18.
[205] Lynch S. Some fractographic contributions to understanding fatigue crack growth. Int J Fatig 2017;104:12–26.
[206] Von Pezold J, Lymperakis L, Neugebeauer J. Hydrogen-enhanced local plasticity at dilute bulk H concentrations: the role of H–H interactions and the formation of local hydrides. Acta Mater 2011;59:2969–80.